The Geological Society of America
Field Guide 21
2011

New investigations of Pleistocene glacial and pluvial records in northeastern Nevada

Jeffrey S. Munroe
Geology Department, Middlebury College, Middlebury, Vermont 05753, USA

Benjamin J.C. Laabs
Department of Geological Sciences, State University of New York–Geneseo, Geneseo, New York 14454, USA

ABSTRACT

The Great Basin of the western United States offers tremendous potential for exploring the response of mountain glaciers and lowland lakes to climate changes during the Last Glacial Maximum (LGM, MIS-2, ca. 22–18 ka B.P.) and subsequent glacial-interglacial transition. The combination of well-distributed alpine moraine records and pluvial lake deposits offers an unparalleled opportunity to develop a more precise understanding of temperature and precipitation changes during the latest Pleistocene and into the Holocene. This field trip provides an overview of recent and ongoing work illuminating aspects of the glacial and pluvial history of northeastern Nevada from the LGM to the present. The route of this trip involves three full days of stops separated by two nights in Elko, Nevada. The first day focuses on glacial deposits at the type locality for the LGM Angel Lake Glaciation on the eastern side of the East Humboldt Range. The second day explores the geomorphic record of pluvial Lakes Franklin and Clover on the east side of the Ruby–East Humboldt Mountains and describes recent efforts to develop a chronology for the late Pleistocene regression of these lakes. The final day again focuses on glacial geology, starting with the type locality of the pre-LGM Lamoille Glaciation on the west side of the Ruby Mountains, and ending with several stops along the scenic drive up Lamoille Canyon.

INTRODUCTION

The Great Basin of the western United States offers tremendous potential for exploring the response of mountain glaciers and lakes to climate changes during the Last Glacial Maximum (LGM) and subsequent glacial-interglacial transition (GIT). Despite the modern arid climate and hot summer temperatures, numerous mountain ranges in the region contain evidence of former glaciers (Blackwelder, 1931; Sharp, 1938; Osborn and Bevis, 2001; Blackwelder, 1934). For instance, the Sierra Nevada, which form the western border of the Great Basin, were extensively glaciated and were one of the first locations in which cosmogenic surface-exposure dating was employed to develop a moraine chronology (Phillips et al., 1996). At the eastern border of the Great Basin, a detailed chronology of latest Pleistocene glaciation has been developed for the Wasatch Mountains (Madsen and Currey, 1979; Lips et al., 2005; Laabs et al., 2007) and glacial records there have been used in numerical modeling exercises

Munroe, J.S., and Laabs, B.J.C., 2011, New investigations of Pleistocene glacial and pluvial records in northeastern Nevada, *in* Evans, J.P., and Lee, J., eds., Geologic Field Trips to the Basin and Range, Rocky Mountains, Snake River Plain, and Terranes of the U.S. Cordillera: Geological Society of America Field Guide 21, p. 1–XX, doi: 10.1130/2011.0021(01).

to yield paleoclimatic inferences (Plummer and Phillips, 2003; Laabs et al., 2006). Yet in contrast to these well-studied ranges at the margins, little is known about the timing of late Pleistocene glacier fluctuations in the interior ranges of the Great Basin, an area covering more than 500,000 km^2. The largest glaciers between the Wasatch and Sierra Nevada were located in the East Humboldt and Ruby Mountains of northeastern Nevada where moraines document the LGM and multiple glacial stillstands during the last GIT (Laabs and Munroe, 2008). Indeed, the last glaciation in the Great Basin was designated the "Angel Lake Glaciation" after well-preserved glacial deposits in the East Humboldt Range (Sharp, 1938). Three pluvial lakes were also present near the East Humboldt and Ruby Mountains during the Angel Lake Glaciation: Lakes Franklin, Clover, and Waring. Although these lakes were small compared with the better-known Lakes Lahontan and Bonneville, their deposits are easily recognized and mapped, allowing their former extents to be delineated (Reheis, 1999). The combination of well-distributed alpine moraine records and pluvial lake deposits offers an unparalleled opportunity to develop a more precise understanding of temperature and precipitation changes during the latest Pleistocene and into the Holocene.

TRIP OVERVIEW

This field trip provides an overview of recent and ongoing work illuminating aspects of the glacial and pluvial history of northeastern Nevada from the Last Glacial Maximum (MIS-2, ca. 22–18 ka B.P.) to the present. The route of this trip involves three full days of stops separated by two nights in Elko, Nevada (Fig. 1). Latitude and longitude coordinates are given for each stop (WGS-84) in the following descriptions as an aid to future users of this guide. The first day of the trip focuses on glacial deposits at the type locality for the LGM Angel Lake Glaciation on the eastern side of the East Humboldt Range. From Logan, we will drive west across the Bonneville Basin in northwestern Utah into Nevada. After reaching I-80, we will continue west over Pequop Summit, across the Independence Valley, and over Moor Summit to the town of Wells. Exiting the highway at Wells, we will follow a winding road up to the valley of Angel Creek and spend the afternoon visiting three closely spaced stops (Fig. 2).

After a night in Elko, Nevada, the second day of the trip explores the geomorphic record of pluvial Lakes Franklin and Clover on the east side of the Ruby–East Humboldt Mountains (Fig. 2). The Franklin Valley is home to the Ruby Lake National Wildlife Refuge, and we will start our day with an overview of the Refuge provided by staff of the U.S. Fish and Wildlife Service. We will then work our way northward from the southern end of the Franklin Valley, stopping to examine localities where the late Pleistocene highstand and other water planes are well expressed. We will also discuss new geochronologic constraints on some of these deposits. In mid-afternoon, we will exit the north end of the former Lake Franklin basin and cross the divide to the Clover Valley that hosted pluvial Lake Clover during the late Pleistocene. Our two final stops will provide an overview of the Lake Clover geomorphic record, including a spectacular series of beach ridges that have been dated by optically stimulated luminescence (OSL) and ^{14}C.

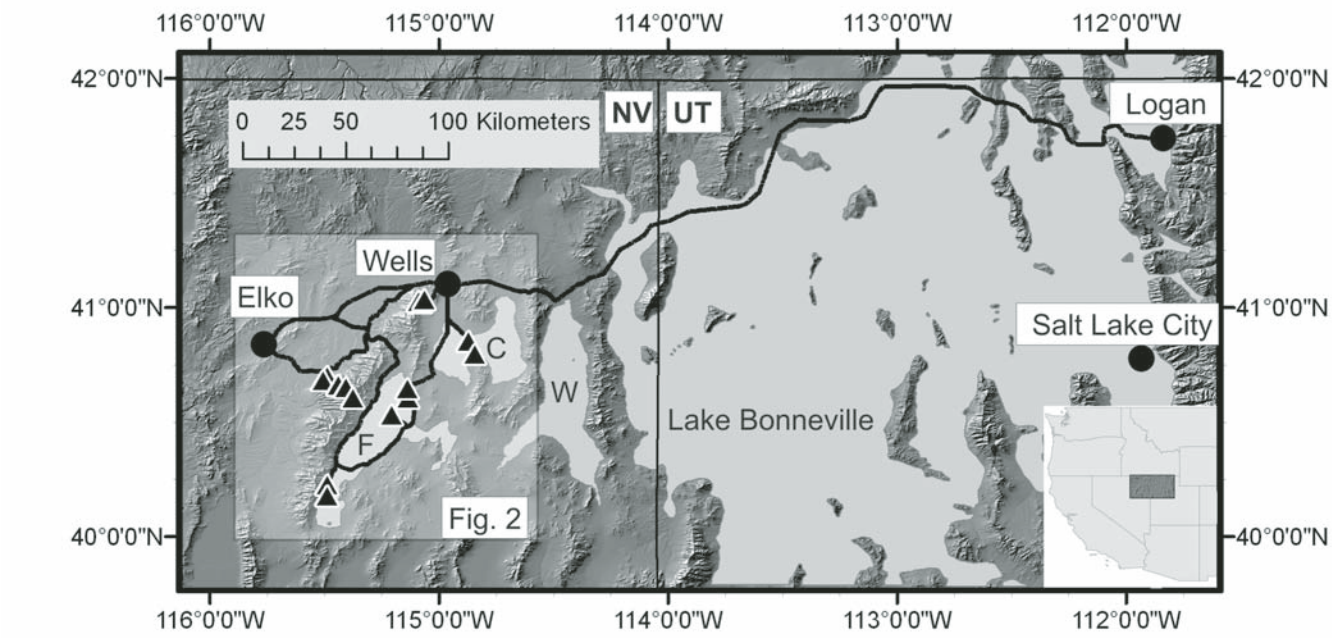

Figure 1. Route of the field trip from Logan, Utah (UT), to northeast Nevada (NV). F—Lake Franklin; C—Lake Clover; W—Lake Waring. Lower right inset shows location of figure in western United States. Shaded box outlines the location of Figure 2.

The final day will again focus on glacial geology, starting with the type locality of the pre-LGM Lamoille Glaciation on the west side of the Ruby Mountains (Fig. 2). Deposits at the mouth of Lamoille Canyon have been assumed to represent an advance during MIS-6, and we will discuss efforts to date these landforms with cosmogenic ^{10}Be surface-exposure dating. We will also hike southward along the range front to Seitz Canyon to visit a spectacularly preserved series of Lamoille and Angel Lake–age moraines that have been the focus of a concerted ^{10}Be dating effort. Our final stops will be along the scenic drive up Lamoille Canyon, a deep U-shaped valley considered the "Yosemite of Nevada." We will discuss the geomorphology of the valley, the distribution of glacial deposits within it, and efforts to identify the moraine from the LGM (i.e., the Angel Lake equivalent moraine in Lamoille Canyon). After lunch at the head of Lamoille Canyon, we will drive northward along the western slope of the Ruby–East Humboldt Mountains to reach I-80 and retrace our route back to Logan.

PHYSICAL SETTING

Northeastern Nevada is the heart of the Great Basin and features classic Basin and Range topography. The relative lowland of the Bonneville Basin, formerly inundated by pluvial Lake Bonneville, ends abruptly at the Utah-Nevada state line, where the landscape takes on an increasingly corrugated appearance moving westward from the border. Long, linear valleys separated by rugged north-south–oriented mountain ranges characterize the area of this field trip. Moving westward from the state line along I-80, one sequentially crosses the Toano Range at Silverzone Pass (1815 m), the Goshute Valley formerly occupied by pluvial Lake Waring, the Pequop Mountains at Pequop Summit (2124 m), the Independence Valley, Moor Summit (1882 m), and the Clover Valley before arriving at the highest mountains in the region, the Ruby–East Humboldt Range. These mountains extend for ~130 km with an orientation of north-northeast to south-southwest. Summit elevations range up to 3471 m at Ruby Dome.

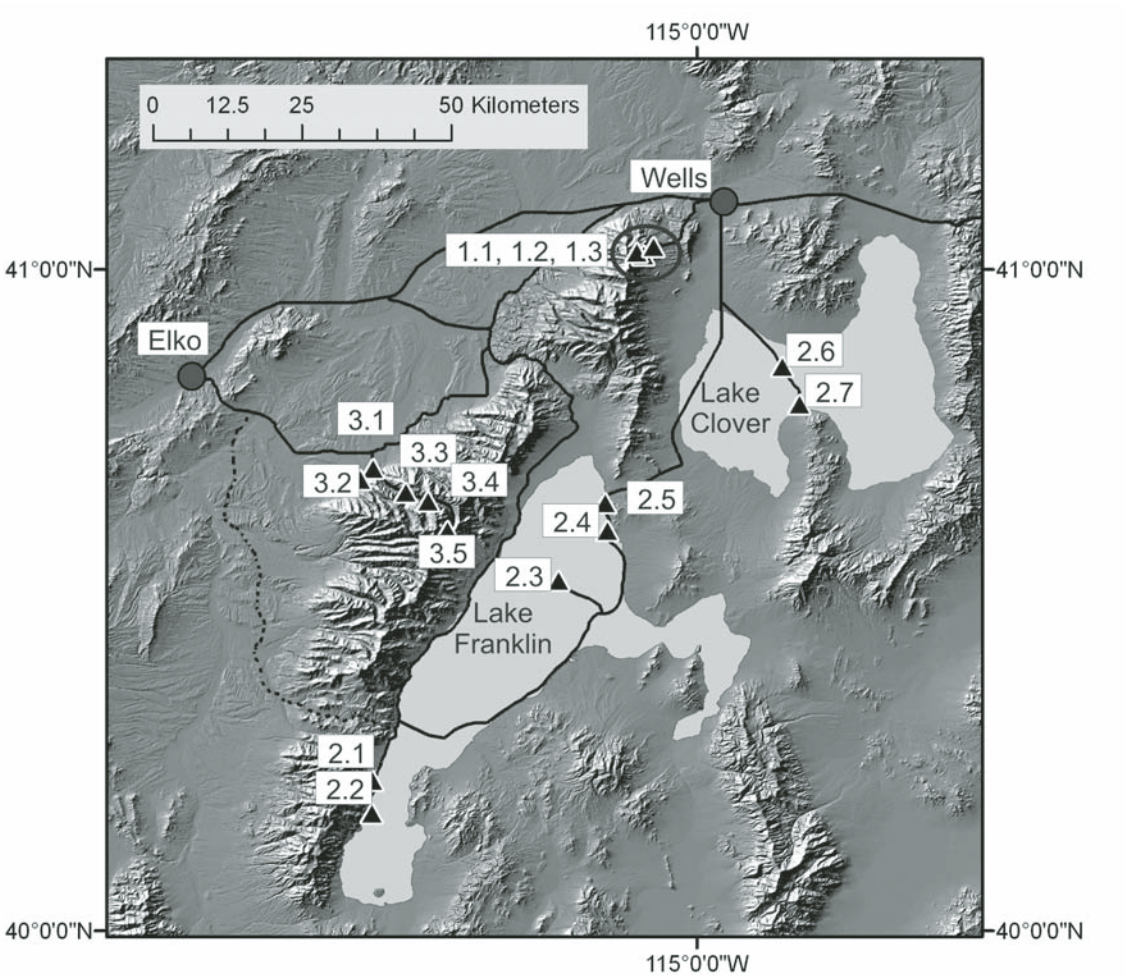

Figure 2. Detail map of field trip stops. Dotted line shows alternate route over Harrison Pass on Day 2. See text for details.

The modern drainage systems in this area are ephemeral, and primarily carry spring snowmelt and precipitation from summer thunderstorms down to evaporate on basin floors. The northwestern end of the Ruby–East Humboldt Range, however, is within the headwaters of the Humboldt River which flows for ~500 km westward across northern Nevada before terminating in the Humboldt Sink. Interstate 80 follows the Humboldt River from near Wells, downstream to the Sink in a broad arc across northern Nevada; however, high mountains with obvious glacial geomorphology are generally absent in this sector of the state.

GLACIAL GEOMORPHOLOGY

Although glaciers are absent from the mountains of northeastern Nevada today, the spectacular upland landscapes, particularly of the Ruby–East Humboldt Range, testify to extensive Pleistocene glaciation. Glaciers formed at the heads of most valleys draining the mountain flanks. Some of these were short and remained confined to their cirques. Others flowed at least some distance downvalley, converting valley cross sections into broader U-shaped profiles. Given the asymmetric nature of the Ruby–East Humboldt uplift, valleys are much steeper on the eastern mountain flank. Glaciers in some of these valleys must have resembled icefalls more than typical valley glaciers. In contrast, glaciers descending the gentler western valley slopes flowed a greater distance from cirque headwalls, but reached similar terminus elevations.

Blackwelder (1931; 1934) presented a short overview of the glacial geology of the Ruby Mountains. In colorful language, he described the "wild crags of the freshly torn cirques" and noted that the glacial deposits represent two glaciations separated by a prolonged interval of weathering. He named these the Lamoille (older) and Angel Lake (younger) glaciations. Sharp (1938) expanded upon Blackwelder's work, formalized the Lamoille and Angel Lake designations, discussed controls over the extent of glaciation, and summarized mechanisms of post-glacial valley modification.

Terminal moraines dating to the Angel Lake Glaciation form bouldery arcuate ridges that cross the floors of most valleys. Streams have cut narrow post-glacial channels through these, but the moraine forms are still obvious. In many settings, multiple crests are present on the overall Angel Lake moraine complex. Older moraine ridges representing the Lamoille Glaciation are found at lower elevations in most valleys. At the type locality at the mouth of Lamoille Canyon, these deposits delineate a piedmont lobe that sprawled outward from the mountain front. In other valleys, particularly along the western slope, Lamoille deposits form steep-sided lateral moraines that project beyond the Angel Lake terminal moraine complex. Other than at Lamoille Canyon, terminal moraines of Lamoille age are not preserved. Downslope from these features, outwash valley trains and meltwater channels are locally well developed.

Recent inventorying of glacial features has supported a comprehensive reconstruction of former glaciers in the Ruby–East Humboldt Mountains. This work indicates that the Ruby–East Humboldt Mountains contained over 130 glaciers during the Angel Lake Glaciation, which collectively covered more than 270 km^2 (Laabs and Munroe, 2008). Reconstructed equilibrium line altitudes (ELAs) range from 2350 to 3000 m, with a mean of ~2700 m. Equilibrium lines generally lowered in elevation from south to north, and 10 of the 15 glaciers with ELAs below 2500 m were located on the western slope. Together, this pattern indicates prevailing moisture transport from the northwest during the Angel Lake Glaciation.

In a comprehensive overview of glacial deposits in the Great Basin, it was noted that Angel Lake moraines are commonly bulky masses of till on valley floors that strongly contrast with the discrete ridges of the remaining Lamoille-age moraines (Osborn and Bevis, 2001). Such voluminous, hummocky moraines are usually produced by glaciers carrying large volumes of sediment. Because Angel Lake moraines typically exhibit this morphology throughout the Great Basin regardless of local lithology, there might be a climatic significance to this observation. Osborn and Bevis (2001) suggested that Angel Lake glaciers may have advanced, retreated, and readvanced multiple times to the same locations, eventually depositing large amounts of till in compound, terminal moraines. In support of this theory, they noted rock flour records from the Owens Valley which reveal multiple millennial-scale intervals of expanded ice in the Sierra Nevada leading up to the LGM (Benson et al., 1998; Bischoff and Cummins, 2001). An alternative possibility is that conditions in the Great Basin were too marginal for extensive alpine glaciation during MIS-4. Instead, this interval was marked by intense periglacial activity that generated large volumes of frost-shattered rubble in the valleys previously occupied by Lamoille glaciers. When the Angel Lake Glaciation began in MIS-2, glaciers transported this backlog of pre-weathered material downvalley to form the anomalously bulky terminal moraines. In contrast, other higher mountain regions in the western United States may have hosted glaciers during MIS-4 that cleaned their valleys down to bedrock. When alpine glaciers again formed and advanced in these valleys during MIS-2, only loose material generated during MIS-3 was available for immediate transport, leading to less voluminous moraines.

PLUVIAL LAKES

Despite the arid climate characterizing the valleys of northern Nevada today, abundant evidence exists for large lakes occupying valley floors in the past. These "pluvial" lakes have been the target of considerable study dating back to the pioneering work of prominent geologists with the U.S. Geological Survey (Gilbert, 1890; Russell, 1885). Features delimiting the former shorelines of these lakes are obvious in dozens of valleys (Reheis, 1999; Mifflin and Wheat, 1979). These include beach berms, cuspate spits, and lagoons at high elevations and featureless plains underlain by deepwater sediment at lower elevations. Mapping and dating of these landforms provides information about former

episodes of lake transgression and regression. Many of these lakes were hydrologically closed (i.e., lacking surface hydrologic connections to other basins), and thus fluctuations in former lake levels are important signals of past climate variability.

The majority of work on pluvial lake records in the western United States has focused on the two largest lakes: Bonneville and Lahontan. At its maximum, Lake Bonneville covered ~50,000 km^2 of western Utah and had a maximum depth of ~300 m (Oviatt, 1997). Lake Lahontan inundated ~22,000 km^2 of interconnected basins in western Nevada and had a maximum depth of ~280 m (Mifflin and Wheat, 1979). The pre–MIS-2 history of both lakes is less precise, but available evidence indicates that lakes were present in these basins multiple times during the Quaternary (Oviatt et al., 1999). In contrast, the MIS-2 deposits of these lakes are well preserved, and abundant evidence indicates that both lakes rose to roughly coincident highstands during MIS-2. Regression continued throughout the latest Pleistocene, and the lakes were reduced to isolated playas and shallow, brackish ponds by the early Holocene (Oviatt et al., 2003).

Despite their fame, Lakes Bonneville and Lahontan were not the only pluvial lakes in the Great Basin. Dozens of smaller lakes existed in valleys from New Mexico northwestward to Oregon, but the records from these settings are much less well understood (Reheis, 1999; Mifflin and Wheat, 1979). This trip in northeastern Nevada will pass through areas formerly inundated by pluvial Lakes Franklin, Clover, and Waring, the first two of which will be topics of numerous stops on Day 2. It is a logical starting assumption that these smaller pluvial lakes rose and fell in concert with Lake Bonneville and Lahonton. However, within this broad chronology, there are numerous details that have been (and remain) important topics for study. One topic is the relative timing of lake highstands across the region. The prevailing theory is that the pluvial climate responsible for the Great Basin lakes was a result of the southward deflection of prevailing storm tracks by the physical barrier imposed by the Laurentide Ice Sheet (Antevs, 1948). This mechanism, which has been broadly supported by numerical modeling (Bartlein et al., 1998), nicely explains the synchronicity between the global LGM and the rising pluvial lakes (Kutzbach, 1987). However, as the chronology of highstands in more basins has improved, a pattern has emerged in which southern lakes reached their highstands and began to regress while northern lakes were still rising (Garcia and Stokes, 2006; Enzel et al., 2003). This regional nonuniformity in lake behavior signifies important regional climatic variability during the last GIT. Most studies have attempted to explain this variability as a function of a northward migrating storm track following retreat of the Laurentide ice margin (Garcia and Stokes, 2006). However, additional work is clearly needed to determine the age of highstands in the numerous basins that remain undated.

Nested within this growing recognition of regionally nonuniform lake behavior during the last GIT is geomorphic evidence for higher frequency climatic variability. Few basins contain just a single emergent shoreline; more commonly, multiple shorelines are preserved, reflecting multiple instances of balanced precipitation and evaporation that stabilized water levels and allowed formation of geomorphically conspicuous shoreline landforms during the overall regressive trend. What was the relative timing of these stillstands among basins? Were they driven by basin-specific factors, such as hypsometry, or do they contain a signal of climate variability during this crucial transition? We will consider these and other questions during our stops in the Franklin and Clover Valleys on Day 2.

DAY 1. LOGAN TO ELKO: THE ANGEL LAKE TYPE LOCALITY

(Total driving distance: ≈290 mi/467 km.)

Day 1 Overview

The first day of this field trip will focus on the region around Angel Lake in the East Humboldt Mountains near Wells, Nevada. Sharp (1938) designated Angel Lake as the type locality of the last Pleistocene glaciation in the Great Basin. Recent work has generated a more detailed view of the distribution of moraines in this valley and has attempted to assign ages to these landforms through cosmogenic ^{10}Be surface-exposure dating. Paleolimnological investigations of sediment cores from Angel Lake have also shed light on Holocene environmental change in this area.

We will drive to Angel Lake from Logan across the extreme northwest corner of Utah. After an early lunch upon arrival at the Angel Creek Campground, we will visit three stops at progressively higher elevations along the road leading up to Angel Lake. Please be prepared for hiking in rough and possibly wet terrain and for sudden changes in weather (temperatures at higher elevations may be close to 0 °C). Late in the afternoon we will continue west for another 45 minutes to Elko, Nevada, where we will spend the night at the Red Lion Hotel.

Directions to Stop 1.1

From the Riverwoods Conference Center in Logan, begin driving west on E 200 N toward N Main Street. Continue on U.S.-30 W toward I-15 S. Take exit 379 off I-15 to merge with I-84 W and travel 36.4 mi to exit 5. Continue on U.S.-30 across northwestern Utah, passing south of the Raft River Range and to the northwest of most of the former Lake Bonneville. At the Utah-Nevada border, U.S.-30 becomes NV-233. *Note that Nevada is in the Pacific time zone; set clocks back 1 hour.* Continue another 34.1 mi to I-80, and head west 27 mi to Wells, Nevada. Take exit 351, turn left under the highway, and then right on Angel Lake Road (NV-231). Follow this road 7.3 mi to the left turn into Angel Creek Campground (Fig. 3).

Stop 1.1. Angel Lake Type Locality (41.02111°N, 115.08025°W)

The drive from Wells, Nevada, toward Angel Lake affords many tremendous views of terminal moraines at the type locale

for the Angel Lake Glaciation (Sharp, 1938). Here, in the northeastern sector of the East Humboldt Range, a 3-km-long glacier constructed latero-frontal moraines that form a nearly continuous terminal moraine loop in the Angel Creek drainage (Fig. 3). As noted by Osborn and Bevis (2001) the moraine crest (at 2317 m) is bouldery, displays low-relief hummocky topography, and has a steep ice-distal slope with ~60 m of relief (Fig. 4). Portions of the distal slope grade to an outwash fan that forms the surface at Stop 1.1. Elsewhere, till comprising the distal slope is inset to older, possibly Lamoille-equivalent moraines with relatively low-relief and few, deeply weathered erratic boulders at the crest.

Along the southern slope of the terminal moraine, a recent breach in the moraine exposes till comprising the landform (Fig. 3). Although the exact origin of the breach is unknown, it apparently formed as a result of headward erosion in a tributary of the North Fork Angel Creek, perhaps aided by drainage of a small lake that may have existed behind the moraine loop. The exposed diamicton bears physical properties typical of sediments comprising alpine moraines; poorly sorted with a coarse-grained sandy matrix, clasts consisting of local lithologies (chiefly granodiorite and gneiss), and clast sizes ranging from pebbles to large boulders. Weathering profiles in the till are evident near the top of this and other exposures, and are consistent with those of Angel Lake–equivalent till elsewhere in the region (Bevis, 1995; Wayne, 1984) and the correlation of the Angel Lake Glaciation to the Wisconsin Glaciation (Richmond, 1986). X-ray diffraction analysis of samples from within the weathering profile reveals the presence of pedogenic kaolinite and vermiculite that are absent in the unweathered till (Rosenberg et al., 2011).

The precise timing of the Angel Lake Glaciation is poorly known throughout much of the Great Basin, due in large part to the lack of numerical age limits on glacial deposits. We are attempting to resolve this issue by applying cosmogenic ^{10}Be surface-exposure dating to the type Angel Lake terminal moraine at this stop and to several other moraines in northeastern Nevada. As noted by Osborn and Bevis (2001), Angel Lake–equivalent moraines typically display bouldery crests; however, in the East Humboldt and Ruby Ranges, many erratic boulders are not suitable for cosmogenic ^{10}Be surface-exposure dating because of their lithology (lacking quartz) or their degree of physical weathering. However, through extensive mapping we have identified numerous erratic boulders suitable for this dating method here and on other moraines in the Ruby and East Humboldt Ranges. Five erratic boulders atop the terminal moraine were sampled, in addition to a suite of boulders from atop the right lateral moraine (Fig. 3; Stop 1.2).

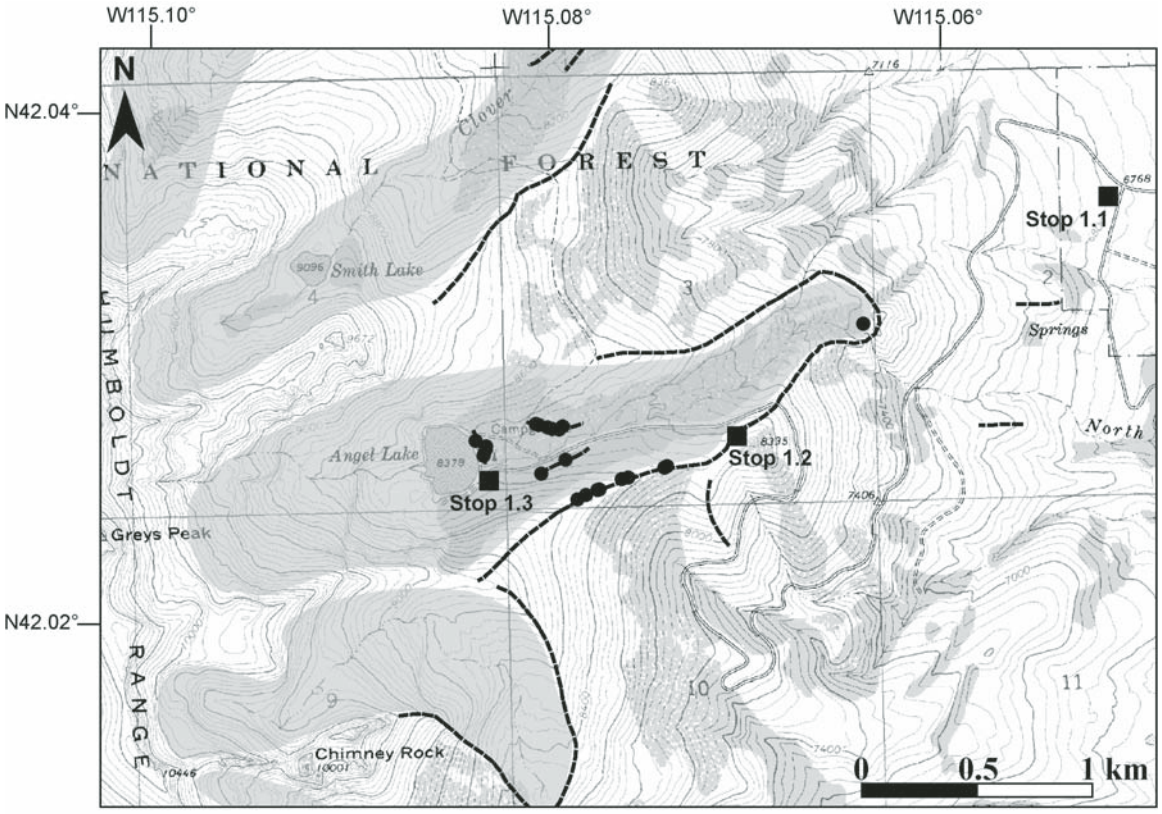

Figure 3. Topographic map of the Angel Lake area (portion of the U.S. Geological Survey 7.5′ Welcome quadrangle), including Stops 1.1, 1.2, and 1.3 (squares). Dashed lines indicate mapped moraine crests, and circles indicate locations of boulders sampled for cosmogenic ^{10}Be surface-exposure dating. Shaded areas indicate the extent of glaciers during the Angel Lake Glaciation.

Before driving to Stop 1.2, note the bouldery surface on the west side of the road just below the break in the distal slope of the terminal moraine. This surface is mapped as Lamoille-age till and is likely part of a moraine that was subsequently buried by till of the Angel Lake Glaciation. This age assignment is based in part on the physical properties of boulders on this surface, which display evidence of intense physical weathering suggestive of prolonged surface exposure.

Directions to Stop 1.2

From Angel Creek Campground, retrace the route out of the campground to Angel Lake Road and turn left (Fig. 3). Follow this road through a series of switchbacks up the mountain front and into the cirque holding Angel Lake. Note that this road is extremely steep, narrow, and winding. Use caution when observing roadcuts, and watch for two-way traffic. Park along the road where it straightens out after the final left turn into the cirque (~3.5 mi from turn out of campground). From the road, climb upslope to the south (left) to the crest of the Angel Lake–age right lateral moraine.

Stop 1.2. Angel Lake Right Lateral Moraine (41.0246°N, 115.09004°W)

The bouldery crest of the right-lateral moraine rises ~35 m above the road and is continuous over a distance of ~0.7 km. It pairs with a left-lateral moraine that is visible to the north across Angel Creek; together, these moraines delimit the vertical extent of the glacier in this valley during the Angel Lake Glaciation (Fig. 3). The frequency of erratic boulders at the moraine crest increases upvalley. Although some of these boulders display clear evidence of substantial surface erosion, many are tall enough and display glacial polish and/or resistant quartz-rich protrusions to render them suitable for cosmogenic ^{10}Be surface-exposure dating. We have sampled ten boulders atop this moraine, and processing of these samples is under way.

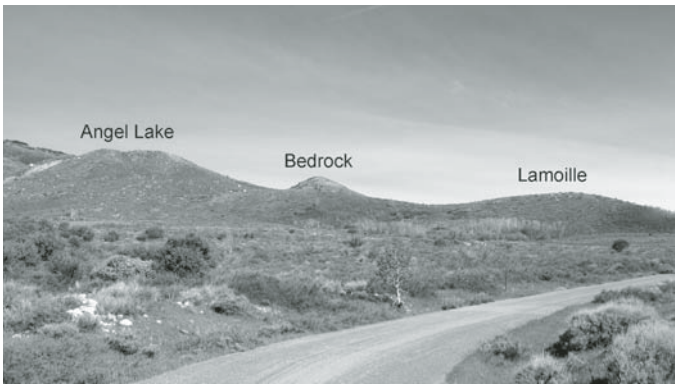

Figure 4. Profile view (to the north) of the Angel Lake and Lamoille terminal moraines from Angel Creek Campground. The Angel Lake moraine is taller, steeper, and more bouldery. The Lamoille moraine is dotted with infrequent, but very large, boulders. The road climbing to Stop 1.2 passes between the two moraines, in front of the bedrock knob visible in the background.

Several additional Pleistocene features are visible from this stop. To the south, a peculiar, bouldery ridge protrudes at a right angle to, and is apparently crosscut by, the right-lateral moraine (Fig. 3). Exposures in this feature along the road indicate that it is composed of till and its surface form suggests that it is a moraine. However, the shape of the glacier that would have constructed this feature is not consistent with the obvious glacier morphology during the Angel Lake Glaciation. Perhaps the Angel Creek glacier flowed southward during a pre–Angel Lake Glaciation to construct this ridge. Alternatively, the ridge may have been constructed by ice in the next valley to the south (South Fork Angel Creek) during a pre–Angel Lake Glaciation.

To the north, a well-preserved sequence of recessional moraines is visible as lower ridges inset to the outermost left-lateral moraine along the axis of the Angel Creek valley. These moraines clearly mark the path of ice retreat after the maximum of the Angel Lake Glaciation, with the youngest, innermost moraine impounding the northeast side of Angel Lake. We sampled boulders atop several of these moraines for cosmogenic ^{10}Be surface-exposure dating (Fig. 3).

Finally, to the southeast, the Clover and Independence Valleys are visible, situated east of the East Humboldt Range. Together these valleys were occupied by pluvial Lake Clover (Fig. 2), which will be explored on the second day of this field trip. Shoreline ridges of Lake Clover, spanning elevations of 1729–1711 m, are best viewed from this stop during the afternoon hours of sunny days. The southern end of the Clover Valley is now occupied by Snow Water Lake, with a mean elevation of 1707 m.

Directions to Stop 1.3

Carefully descend the proximal moraine slope to the road, and drive the remaining stretch up to the final parking lot (straight ahead after the cattle guard). Park the vehicles and walk a short distance to the dam impounding Angel Lake (Fig. 3).

Stop 1.3. Angel Lake (41.03380°N, 115.06502°W)

Angel Lake is a natural tarn at 2554 m that was slightly enlarged by a dam built in the early 1900s. The setting is quite scenic, and that quality combined with the easy access from Wells and I-80, makes this a popular spot. Snow melting higher in the cirque during early summer feeds an impressive cataract that enters the lake opposite the dam. A tremendous headwall rising 700 m to Greys Peak encircles the lake on three sides, while a pair of steep-sided lateral moraines extends eastward from the lake along the road. In early summer, the water level is quite high on the dam, but it falls ~2 m as water is released, forming a narrow sandy beach as the summer progresses.

From a glacial geology perspective the lake is located at the young end of a well-preserved series of moraines (Fig. 3). The outermost moraines of presumed Lamoille age were viewed at

Stop 1.1, while the classic Angel Lake moraines were seen from Stops 1.1 and 1.2. Other recessional moraines are clearly visible from the road leading up to the dam, and remnants of inset lateral moraines extend toward the valley axis near the campground as well as on the south side of the road. The youngest end moraine loops down from the north side of the cirque and partially encloses the lake; the artificial dam extends this natural ridge across to the south side to raise the original water level slightly.

The position of Angel Lake inside the innermost recessional moraine indicates that the sedimentary record from the lake should contain information about environmental changes occurring in this area since deglaciation. To investigate this record, the lake was cored in June 2007. To select the coring location, a bathymetric map was first created from over 300 depth measurements fixed with a GPS receiver (Fig. 5). The lake has a maximum depth of 11 m, a mean depth of 6.5 m, an area of 53,000 m^2, and a volume of 346,000 m^3. The watershed area-lake area ratio is 25:1, and assuming a uniform annual precipitation of 0.89 m/yr (measured at the Hole in Rock SNOTEL site less than 10 km away at a similar elevation on the same side of the range), the flushing rate of the lake is 3.5 times/yr.

The bathymetric map (Fig. 5) reveals a deep hole just offshore from the main fluvial input at the western side of the lake. Because the goal was to retrieve a long, undisturbed record, it was decided to core to the east of the deep hole in slightly shallower water so that episodic flooding events that might deliver large amounts of coarse, reworked sediment to the lake, would not overwhelm the sedimentary record. Care was also taken not to core too close to the dam in case this area was dredged during dam construction. Coring was completed from an anchored platform using a Livingstone corer for the loose surface sediment, and a percussion corer for deeper material. The cores were retrieved in 9.14 m of water, and the composite record extended from the sediment-water interface to a depth of 4.54 m below the lake bottom. The basal sediment of the percussion core contains disseminated shards of tephra, and OSL analysis returned an age (7.94 ± 0.9 ka B.P.) consistent with the Mazama eruption. That constraint, along with 5 accelerator mass spectrometry radiocarbon dates, supports a depth-age model that spans ~7.7 ka B.P. (Fig. 6).

Back in the lab, multiple proxies were investigated at 1-cm intervals including: water content, loss-on-ignition (LOI), C:N ratio, biogenic silica content, and grain size distribution (Munroe and Laabs, 2009). LOI and water content show significant transient departures from an overall increasing trend through the record (Fig. 6). Biogenic silica and LOI values are notably above average from 1 to 2 ka B.P. and ca. 7 ka B.P., suggesting a warmer, more productive lake environment. These episodes

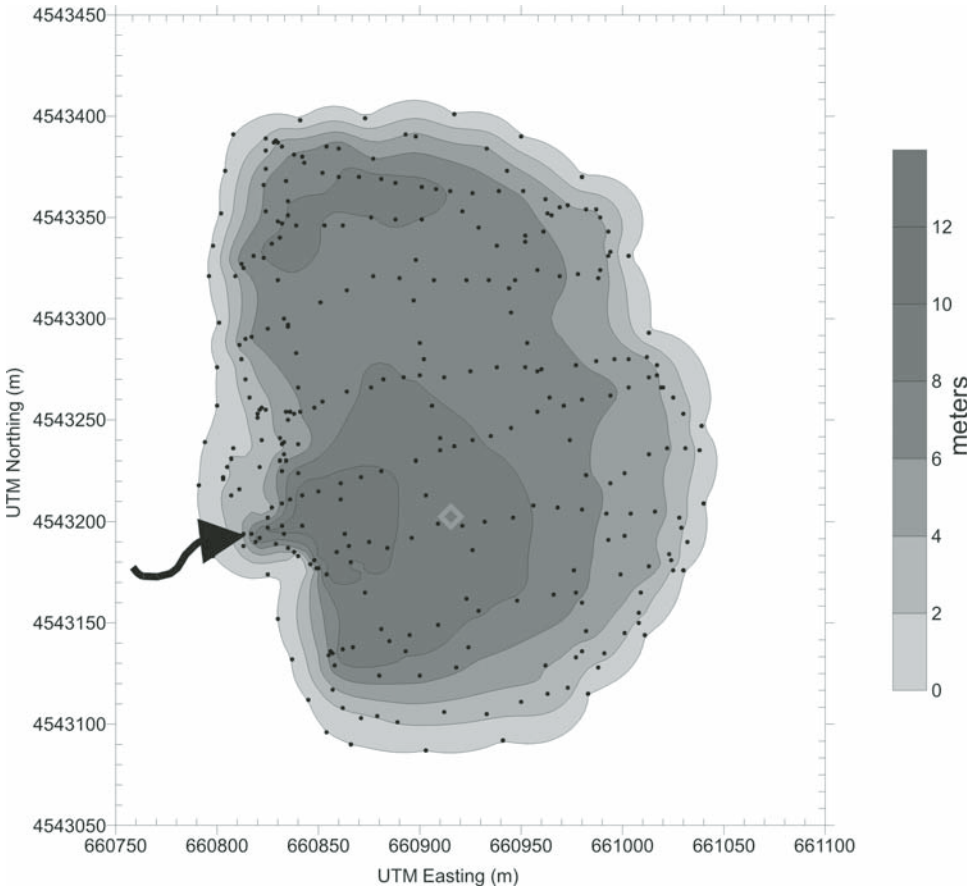

Figure 5. Bathymetric map of Angel Lake with depths in meters. Map was created from ~300 GPS-linked depth measurements. The location of the 2007 core is shown by the diamond near the center, just east of the deep hole near the western inlet (arrow).

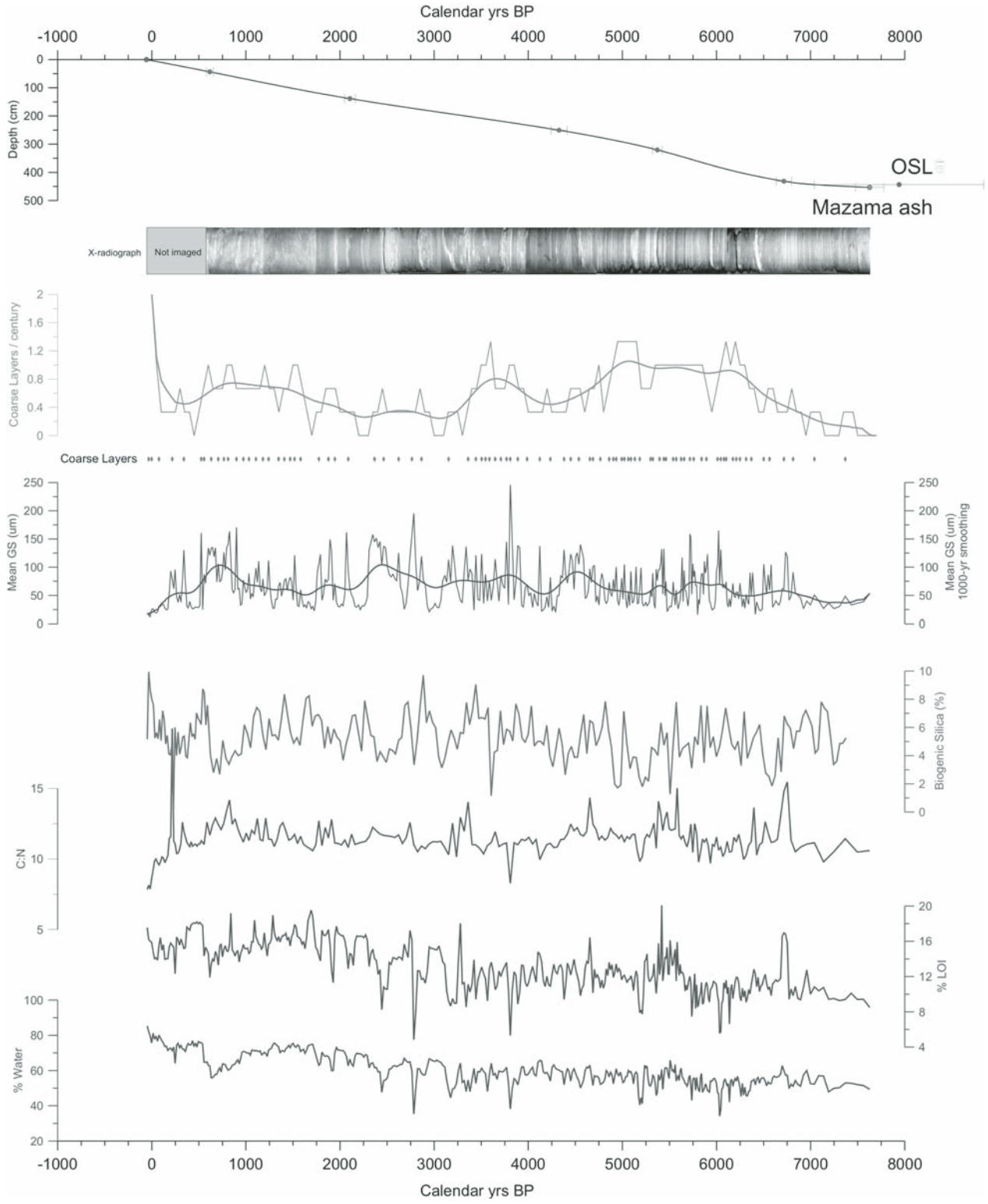

Figure 6. Multiproxy time-series from the Angel Lake core. Water content rises through the record reflecting compacting of sediment over time. Loss-on-ignition (LOI, a proxy for organic matter content) also rises, with significant departures from this overall trend. C:N ratio varies reflecting the relative input of terrestrial versus aquatic debris. Biogenic silica values vary widely, perhaps reflecting changes in summer water temperature and/or duration of the ice-free season. Mean grain size (GS) is also highly variable. The analysis described in the text yielded an objective identification of coarse layers inferred to record wet avalanches onto the lake ice. The frequency of these events was highest in the middle Holocene, and ca. 3500 and 1000 yr B.P. The thicker coarse layers are visible as light gray bands on the X-radiograph. The depth-age model was based on five accelerator mass spectrometry ^{14}C dates, the year A.D. 2007 for the core surface, the presence of tephra assumed to be from the Mazama eruption near the base, and an optically stimulated luminescence analysis on the basal sediment.

of increased productivity are broadly consistent with times of increased chironomid-inferred July air temperatures at Stella Lake in Great Basin National Park, 250 km to the south (Reinemann et al., 2009). In particular, the interval of peak warmth at Stella Lake ca. 5.5 ka B.P., is synchronous with an interval of particularly high LOI values (Fig. 7). Higher LOI values in the later Holocene overlap with times of reconstructed high water levels in Ruby Lake to the southeast, as well as Pyramid Lake and Lake Tahoe at the western end of the Great Basin (Fig. 7). Together these similarities suggest a general increase of both relative moisture and productivity in high-elevation lakes in the late Holocene.

Mean grain size in the Angel Lake record is highly variable, with spikes to locally high values reflecting delivery of clastic debris to the coring site by high-energy events (Fig. 6). One possible interpretation is that these coarse layers represent floods on the inlet stream draining into the lake. However, because the core was retrieved from the opposite side of the depocenter from the inlet in water ~2 m shallower than the deepest part of the basin, it is unlikely that these clastic layers are evidence of direct fluvial inputs. Instead, these layers are interpreted to represent depositional events during the winter and spring when run-out from snow avalanches and slushflows could travel across the ice to the coring site (Munroe and Laabs, 2009). To objectively identify these discrete events in the record, a Gaussian smoothing function was run through the grain size time series and avalanche events were defined as peaks rising above the local background level. Results from this analysis indicate that the frequency of avalanches was below average from 1.8 to 3.2 ka B.P., which overlaps the extended low in LOI. In contrast, avalanches were quite common, up to 2 times the long-term average, from 0.5 to 1.5, 3.2 to 3.8, and from 4.5 to 6.5 ka B.P. The oldest interval is synchronous with a prolong interval of warm temperatures at Stella Lake, as well as lowstands in Ruby Lake, Pyramid Lake, and Lake Tahoe (Fig. 7). Together these fluctuations may reflect changes in winter/spring moisture delivery to the northeastern Great Basin. Alternatively, increases in avalanche frequency may indicate more common rain-on-snow events or episodes of rapid warming during the spring thaw, both of which could stimulate wet avalanches and slushflows.

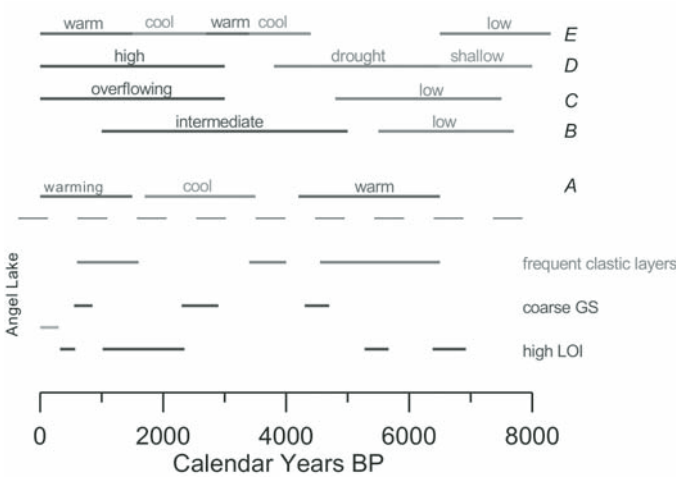

Figure 7. Comparison of Angel Lake record with other records from the region. A—Stella Lake in Great Basin National Park (Reinemann et al., 2009); B—Ruby Lake (Thompson, 1992); C—Lake Tahoe (Benson et al., 2002; Lindstrom, 1990); D—Pyramid Lake (Benson et al., 2002); E—Blue Lake (Louderback and Rhode, 2009). Intervals of high loss-on-ignition (LOI) at Angel Lake generally line up with times of warm temperatures at Stella Lake in Great Basin National Park. High LOI also corresponds to a greater frequency of clastic layers. Intervals of fine grain size (GS) are out of phase with high LOI. See text for discussion.

Directions to Elko

Return to I-80 via the Angel Lake Road (NV-231). Use caution on the steep descent, particularly if driving a fully loaded van. Use of lower gear is recommended in order to prevent brakes from overheating. Pass under the highway and turn left to access I-80 westbound. Travel 47 mi to Elko and take exit 303. Turn left under the highway, then right on Idaho Street. Turn right into the Red Lion Hotel.

DAY 2. ELKO TO ELKO: PLUVIAL LAKES FRANKLIN AND CLOVER

(Total driving distance: ≈217 mi/350 km over Harrison Pass, 247 mi over Secret Pass.)

Day 2 Overview

Day 2 focuses on the record of pluvial Lakes Franklin and Clover on the east side of the Ruby–East Humboldt Mountains (Fig. 2). We will visit several sites illustrating aspects of the last highstand and regression of both lakes, and will receive an overview of the Ruby Lakes National Wildlife Refuge from Refuge staff (Fig. 8).

Directions to Stop 2.1

From the Elko Red Lion hotel, there are two options for reaching the Ruby Valley. The first is to head south along the west side of the Ruby Mountains before crossing into the Franklin Valley at Harrison Pass. This route is shorter, but the Harrison Pass Road is steep and winding, and parts of it are unpaved, so it may not be possible to cross there in late May. The alternative route is 30 mi longer, but ascends gentler grades to cross the range at Secret Pass, and remains on paved roads. For the purpose of flexibility, and to aid future users of this guidebook, both sets of directions to Stop 2.1 are presented here.

Harrison Pass Route to Ruby Lakes National Wildlife Refuge (62 mi): Turn right on Idaho Street from the Red Lion Hotel. Turn left on 5th Avenue and follow south across the Humboldt River. Continue to follow 5th Avenue as it curves left and becomes NV-227 toward Spring Creek. After ~7 mi, turn right at the light on NV-228. Follow this road south for 30 mi along the western side of the Ruby Mountains through Jiggs and then veer left toward Harrison Pass. Climb toward the pass on U.S. Forest

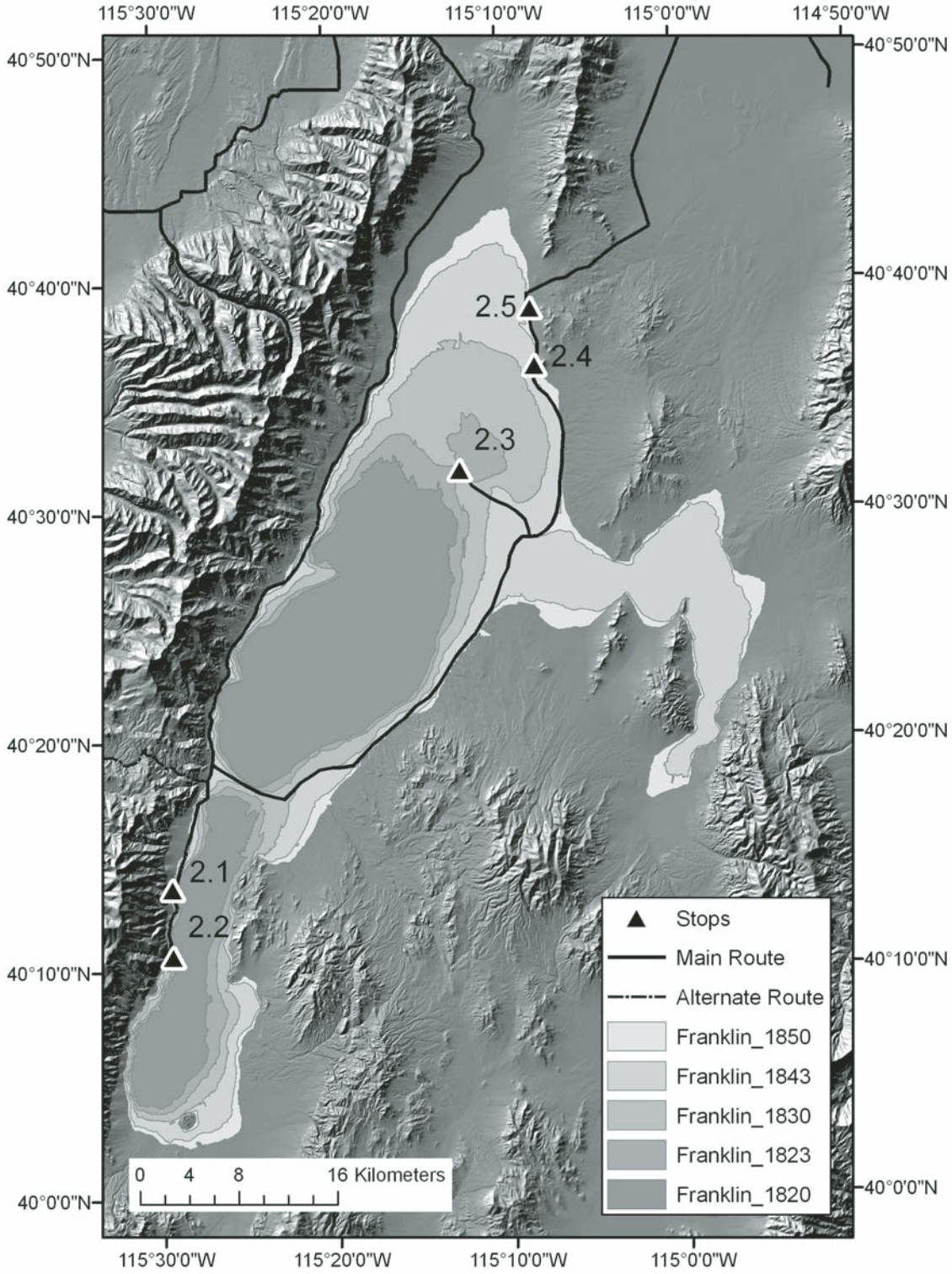

Figure 8. Map of the Lake Franklin region with outlines of the lake at five different elevations (in meters). Field trip stops are identified, and the route of the trip (from Fig. 2) is shown.

Service (USFS) Road 113. Note that the last few switchbacks on this road are unpaved, and the road is not maintained in the winter. A pull-out on the right in Harrison Pass provides a nice view of a landscape featuring eroding outcrops of the Oligocene Harrison Pass Pluton (Howard, 2000). To the east, the Franklin Valley is visible. Descend the east slope of the Ruby Mountains in a narrow canyon and reach Ruby Valley Road at the base of the mountains. Turn right for the Ruby Lakes National Wildlife Refuge (Fig. 8).

Secret Pass Route to Ruby Lakes National Wildlife Refuge (92 mi): Turn left on Idaho Street from the Red Lion Hotel, make the first left on East Jennings Way, and then a quick right to enter I-80 eastbound. Travel 17.6 mi east to exit 321 and follow NV-229 toward Ruby Valley. This road leads over Secret Pass between the northern end of the Ruby Mountains and the southern end of the East Humboldt Range. After 35.6 mi from I-80, continue straight on NV-767 (Ruby Valley Road) along the base of the eastern slope of the Ruby Mountains. This road will meet the route coming over Harrison Pass, and continuing straight will lead to the Ruby Lake National Wildlife Refuge (Fig. 8). The headquarters of the Refuge is on the right ~9 mi south of the intersection of the two routes along a well-maintained dirt road.

Stop 2.1. Ruby Lake National Wildlife Refuge and Pluvial Lake Franklin (40.22654°N, 115.48932°W)

The Ruby Lakes National Wildlife Refuge (RLNWR) was established in 1938 because of its critical location at the crossroads of several major corridors for migrating birds. Today the refuge covers ~40,000 acres, almost half of which is wetlands of the Ruby Marshes. More than two hundred natural springs at the base of the Ruby Mountains deliver water to the marshes, and the Refuge staff manages water levels within different sections of the marsh with a system of dikes, pumps, and canals. A self-guided auto-tour passes through the marshes along several of these dikes, providing abundant opportunities for birdwatching. Maps of the auto tour route are available at the Refuge headquarters. The nearby Gallagher State Fish Hatchery also takes advantage of the water from the springs. The hatchery, which was built in 1940 and substantially updated in the late 1960s, primarily raises trout that are stocked in lakes and streams around northern Nevada.

The RLNWR occupies a valley that formerly held pluvial Lake Franklin, one of the largest pluvial lakes in the Great Basin after Bonneville and Lahontan (Mifflin and Wheat, 1979). At its highest level (~1853 m) Lake Franklin inundated the RLNWR with over 35 m of water, covered more than 1000 km^2, and extended northward through the Franklin Valley, eastward across Dry Lake Flat, and into the North Butte Valley (Fig. 8). All that is left of Lake Franklin today is the shallow Ruby Marshes and an ephemeral lake on the floor of Franklin Valley.

As is the case with most pluvial lakes other than Bonneville and Lahontan, the record of Lake Franklin has received only limited attention. Shoreline features recording a highstand of Lake Franklin were noted by the earliest geological explorations in the area, but were inaccurately considered evidence of a much larger lake (Simpson, 1876). Later expeditions correctly realized that these features reflected a lake in the Franklin Valley (Gilbert, 1890; Russell, 1885). Several decades later, the name Lake Franklin was assigned to this pluvial lake, taken from the modern ephemeral lake on the floor of the Franklin Valley (Sharp, 1938).

Despite this early recognition, only two studies have focused specifically on the history of Lake Franklin and attempted to develop chronologies of its former fluctuations. The first used lacustrine sediment cores from the vicinity of the Ruby Marshes to reconstruct the past 40,000 years of water level changes (Thompson, 1992). Thompson (1992) studied two cores: one drilled to a depth of >7 m at the edge of the modern marsh, and another collected in ~2 m of water just offshore from the first coring site. By comparing the relative abundance of different aquatic palynomorphs, Thompson was able to reconstruct how salinity of the marshes had changed over time, which was considered a signal of water depth. The overall conclusion is that relative fresh and deep water covered the coring site between ca. 18,500 and 15,400 ^{14}C yr B.P. These dates calibrate to ca. 24,500–19,500, and 20,100–16,700 calendar yr B.P., suggesting that the highstand of Lake Franklin was synchronous with MIS-2 and occurred during the final rise to the Bonneville highstand in the Bonneville Basin (Oviatt et al., 1992).

A more complete investigation of the history of Lake Franklin was completed as a Ph.D. dissertation at the University of Utah (Lillquist, 1994). Lillquist (1994) undertook extensive mapping of shoreline features within the area flooded by Lake Franklin, and was able to assign ages to many of these shorelines through radiocarbon dating of shell fragments retrieved from natural exposures and artificial excavations in beach ridges and adjacent lagoons. Lillquist (1994) also recognized several significant shorelines created by Lake Franklin at elevations below the highstand, and constructed a hydrograph charting several cycles of lake regression and transgression during the overall desiccation of the lake from MIS-2 into the Holocene (Fig. 9). The highstand of Lake Franklin at 1853 m is constrained in Lillquist's hydrograph by a pair of dates on shells retrieved from auger holes drilled in lagoons. These dates indicate that Lake Franklin built its highest shoreline between 16,800 ± 130 and 15,070 ± 100 ^{14}C yr B.P. (20,000–18,300 yr B.P. Note: for clarity all calibrated dates are reported as the midpoint of the most probably 2-σ calibration range). A date of 15,020 ± 240 ^{14}C yr B.P. from a small quarry directly in a beach ridge indicates that water level had fallen to 1843 m by 18,200 B.P. A significant regression to ~1823 m occurred by 14,650 ± 340 ^{14}C yr B.P. (17,800 B.P.) based on evidence exposed at the Franklin River Bridge (Stop 2.3). Lake level rose again after this time reaching 1836 m and then 1840 m, with a brief regression to 1826 m in between. The final regression of the lake began at the 1840 m shoreline ca. 12,720 ± 110 ^{14}C yr B.P. (15,000 B.P.), and the last pair of shorelines was constructed at ~1820 m by 11,500 ^{14}C yr B.P. (13,000 calibrated B.P.) (Lillquist, 1994).

The work of Lillquist (1994) is significant for the perspective it provides on lake level dynamics during the last GIT: clearly,

Lake Franklin didn't regress monotonically from its 1853 m highstand. But as noted earlier, the import of these lake level oscillations during overall regression is unclear. What magnitude of climate changes do they represent? Do they reflect the effects in the Franklin Valley of a regional climate forcing, or were they driven by something more local and basin-specific? Did these changes occur synchronously with climate shifts during the last GIT elsewhere in the Great Basin? Ongoing research by the authors is intended to address these questions by further developing the chronology of Lake Franklin fluctuations, and comparing it with records from the unstudied pluvial Lake Clover, as well as glacial moraines deposited during the Angel Lake Glaciation and subsequent deglaciation.

Directions to Stop 2.2

Continue south from the Refuge headquarters past the Gallagher State Fish Hatchery and turn left on (gravel) Brown Dike road (Fig. 8). Park on the right and walk a short distance down into the RLNWR gravel pit for Stop 2.2.

Stop 2.2. Ruby Lake National Wildlife Refuge Gravel Pit (40.17722°N, 115.48968°W)

Please note that the pit is not open to the public. Visitors wishing to view the sediment exposed at this location should check with RLNWR staff at the Refuge headquarters before entering the pit.

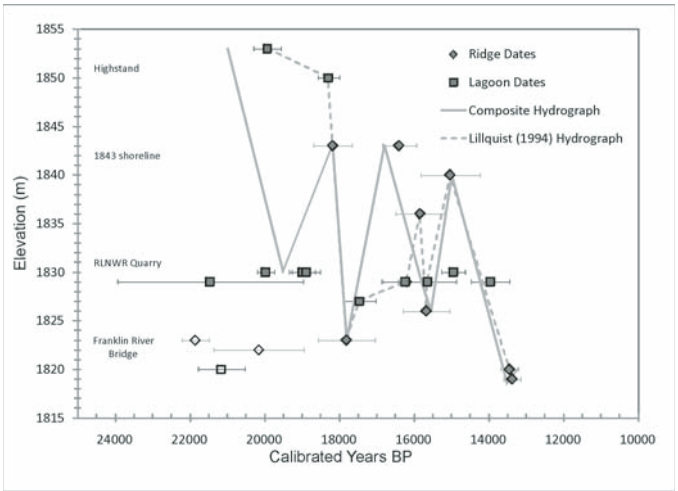

Figure 9. Radiocarbon dates for shorelines of Lake Franklin. The hydrograph of Lillquist (1994) is shown, along with a revised composite version taking into account newly acquired radiocarbon dates. Dates directly from beach ridges are shown as diamonds, while (minimum-limiting) dates from lagoons are shown as squares. Open symbols represent dates on reworked material not used in constructing the hydrographs. Elevations of the highstand, the 1843 m shoreline, the Ruby Lake National Wildlife Refuge (RLNWR) quarry, and the Franklin River Bridge site are noted.

The excavation at this stop was a source of fill used in creating roads and dikes within the RLNWR. The pit is located within a compound spit formed by transport of sediment by waves and currents when Lake Franklin stood at the 1830 m level, ~23 m below the highstand elevation (Fig. 8). The spit projects east-northeast from the mountain front and is bordered to the southwest by a large alluvial fan draining off the southern Ruby Mountains. Lillquist (1994) inferred that the fan served as a major source of sediment for the spit, and concluded that northward sediment transport was dominant, with a minor component of transport to the south and east.

The north wall of the quarry exposes ~4 m of well-rounded, crudely stratified gravel and coarse sand (Fig. 10). The sediment is moderately well indurated and is locally abundantly fossiliferous. Lillquist (1994) interpreted these sediments as a series of lagoon and foreshore/beach units, with the lagoons represented by marly silty sands and the beaches by marly sandy gravels. Changes in the exposure over time due to continued excavation make it impossible to determine exactly how the modern exposure relates to that described by Lillquist (1994). However, the exposure in 2010 was dominated by a coarser facies of indurated gravelly sand, suggesting that it was located solidly in the former beach environment, rather than in a lagoon.

Lillquist (1994) reports three previously unpublished radiocarbon ages from this site collected by D.R. Currey and B.G. Bills. These ages on shells, tufa, and marl from lagoonal environments within this spit complex, range from 12,030 ± 140 ^{14}C yr B.P. (13,960 B.P., shells) to 18,030 ± 1050 ^{14}C yr B.P. (21,460 B.P., marl). In addition to these, Lillquist (1994) reported ages of 14,360 ± 150 ^{14}C yr B.P. (17,500 B.P.) and 12,870 ± 140 ^{14}C yr B.P. (15,650 B.P.) on shells from lagoonal facies at this site.

Figure 10. Exposure in the north wall of the Ruby Lake National Wildlife Refuge gravel quarry in June 2010. The face stands ~4 m high and exposes cross-bedded, indurated, coarse gravelly sand interpreted as a beach environment. Shells dated from this section constrain the elevation of Lake Franklin to 1830 m between 20,000 and 19,000 yr B.P.

In 2010, the authors obtained two more accelerator mass spectrometry radiocarbon analyses on gastropods collected directly from upper and lower sections of the beach gravels exposed in the north wall of the pit. The ages on these samples are 15,750 ± 140 and 16,750 ± 70 ^{14}C B.P. These ages, which are in stratigraphic order, calibrate to ca. 19 and 20 ka B.P., respectively. Dates on shell material from lagoons should be viewed as providing a minimum limiting age on formation of the neighboring ridge because, as Lillquist (1994) notes, the lagoon could remain a locally moist environment capable of harboring mollusks long after the water level has dropped from the level of the ridge. In contrast, dates on shells recovered directly from a beach ridge provide a more direct constraint on the age of the highstand responsible for ridge formation. Viewed in this way, the two new dates for the RLNWR indicate that the water level in Lake Franklin stood at ~1830 m ca. 20–19 ka B.P. The younger dates obtained from this section by Currey, Bills, and Lillquist were all from lagoonal facies, which could have held water at later times when the main lake rose and fell again below the 1830 m level.

The two new dates from the RLNWR quarry require a change in the Lake Franklin hydrograph developed by Lillquist (1994). At first glance, the results from the RLNWR quarry and Lillquist's two sites constraining the Lake Franklin highstand appear incompatible because they suggest the water level was at 1853 m and 1830 m simultaneously. On closer inspection, however, an explanation is revealed by the fact that Lillquist's dates for the highstand are from lagoons, which as noted earlier should be viewed as minimum limiting ages. Combining the dates from lagoons behind the highstand beach ridge and the new shell dates directly from the ridge at the RLNWR quarry, it appears that the highstand of Lake Franklin occurred earlier than Lillquist (1994) suggested, perhaps closer to 21 ka B.P. before the water level fell to the 1830 m level by 20–19 ka B.P. (Fig. 9). This interpretation places the Lake Franklin highstand solidly in the middle of MIS-2, and also aligns cleanly with the duration of the highstand inferred by Thompson (1992). Interestingly, a drop (~40 m) in the elevation of Lake Bonneville known as the Keg Mountain Oscillation has been reported from approximately the same time as the drop in Lake Franklin to the 1830 m level (Oviatt et al., 1992; Burr and Currey, 1988; Currey and Oviatt, 1985).

Directions to Stop 2.3

Turn vehicles around, return to Ruby Valley Road, and head back to the north (right) to exit the Refuge. A quarter-mile past the intersection with the Harrison Pass Road coming in from the left, turn right on the CCC Road (Fig. 8). This dirt road leads along the crest of a narrow ridge that separated Lakes Franklin and Ruby when the water level fell below ~1830 m. Lillquist (1994) inferred that this segmentation feature formed through simultaneous eastward progradation of a spit from the western shore of the lake, and westward progradation of the alluvial fan emanating from Ruby Wash on the eastern shore. This interpretation is based on the overall geomorphology of the feature, as well as the dominance of granitic lithologies derived from the Ruby Mountains in the western half of the ridge, and carbonates from the Maverick Springs and Medicine Ranges in the eastern half.

The main road, which is easy to follow, leads across to the east side of the valley, then turns northward and follows the 1830 m shoreline around the distal end of the large Ruby Wash fan. The road then rises up to the higher shorelines at 1843 and 1850 m and curves back around to the north. Continuing around the west side of the Dry Lake Flat, the CCC Road follows a substantial compound ridge with a crest elevation between 1843 and 1846 m. Lillquist (1994) notes the presence of superimposed shoreline features on this ridge, suggesting that the water level reached this elevation on more than one occasion. The road once again curves to the north near Murphy Well where Lillquist (1994) obtained his highest radiocarbon date directly from a beach ridge (18,200 yr B.P. at 1843 m). Watch for a sign marking the road to Franklin River Bridge on the left ~26 mi after turning onto the CCC Road. Take this turn and follow 6 mi to the site of the former bridge (now impassable). Park along the road on the east side of the bridge for Stop 2.3.

Stop 2.3. Franklin River Bridge (40.52899°N, 115.20827°W)

At this stop, we will review geomorphic and stratigraphic evidence for a major regression in Lake Franklin following the formation of the 1843 m shoreline. The road leads from this shoreline to the Franklin Bridge site across the eastern half of a broad ridge that cuts off the northern part of the Lake Franklin Basin. Lillquist (1994) interpreted this ridge as a compound spit/bayhead bar that has been breached by the combined flow of Withington Creek and the Franklin River. Lillquist (1994) described an exposure of the stratigraphy at this site as ~100 cm of gravelly sand unconformably overlying 50 cm of fine clay, over 50 cm of clayey sand. The fine clay, which contains ostracodes and mollusk fragments, was interpreted as a deepwater deposit, and the overlying gravelly sand as a beach. A date of 14,650 ± 340 ^{14}C yr B.P. (17,800 B.P.) from the base of the gravelly sand provides a constraint on the timing of the lowstand responsible for the beach. Lillquist (1994) reported two other dates from this section: 7320 ± 90 ^{14}C yr B.P. (8150 B.P.) from carbonate concretions in the lowest clayey sand, and 16,880 ± 510 ^{14}C yr B.P. (20,156 B.P.) from an extended counting analysis on small shell fragments from near the top of the section. The lower date is clearly too young and likely represents the time of formation of the concretions, rather than deposition of the sediment. The upper date is out of stratigraphic order, and given the fragmented nature of the shells, likely represents reworking of older shells from a higher shoreline down to the Franklin Bridge site by the Franklin River at the time of the lowstand.

In 2010, the exposure revealed ~150 cm of coarse, gravelly sand unconformably overlying a sticky fine silty loam with 13% clay (Fig. 11). The authors obtained a date of 18,300 ± 95 ^{14}C yr B.P. (21,850 B.P.) on shells from the gravelly sand, 145 cm below the modern surface. We interpret this as additional evidence of

reworking of older material downstream to the location of this beach. As a cross-check on this interpretation, we also collected a sample for OSL dating from the same layer where we dated shell fragments. Results from this analysis should provide some clarification of the mixed ages from this site.

The importance of this regression to the Franklin River Bridge site is unclear; however, it is obvious that the climate changed significantly to reduce the area and volume of the lake so dramatically. Calculations in a geographic information system (GIS) reveal that Lake Franklin lost 53% of its area (1000–467 km^2) and 89% of its volume (17–2 km^3) during the drop from the 1843 shoreline (ca. 18,200 B.P.) to the Franklin Bridge (ca. 17,800 B.P.).

Following this lowstand, the lake elevation rose again, returning to the 1843 m shoreline by ca. 16,800 B.P., given a new date of 13,400 ± 75 ^{14}C yr B.P. (16,400 B.P.) obtained by the authors on a beach ridge in Ruby Wash. This submergence of the bayhead barrier/spit at Franklin River Bridge was likely responsible for the muted form and broad appearance of the feature today. Auger excavations west of the bridge and south of the road reveal ~20 cm of fine silt overlying coarse, rounded gravel which may represent deeper water sediments that accumulated over the beach facies during this transgression. Reoccupation of the 1843 m shoreline is consistent with the presence of superimposed beach features at the 1843 m level noted by Lillquist (1994). The 1843 m shoreline marks the general elevation of the division between the main Franklin Valley and the North Butte–Dry Lake Flat sections of the basin. Lillquist (1994) suggested that spillover of water from the Franklin Valley into these basins to the east could have helped maintain the lake at this elevation. Calculations in a GIS support this interpretation. The area of Lake Franklin at the 1843 m elevation was 1000 km^2, but 140 km^2 of that was contained within the shallow arm extending east into the North Butte Valley (Fig. 8). Thus, the rise of the lake from just below, to just above, the 1843 m level involved an instantaneous increase in surface area of 16%. Such a substantial increase in area available for evaporation could have exerted a strong limiting influence on continued water level rise.

Figure 11. Stratigraphic section exposed at the east end of an excavation east of the Franklin River Bridge in June 2010. The section exposes ~100 cm of bedded, fossiliferous, coarse sandy gravel interpreted as a beach deposit. This unit sits unconformably on a silty-clay layer (not shown) interpreted as a deep-water facies. Shell samples were collected from the beach gravel (near tip of shovel handle) and a shielded sample for optically stimulated luminescence analysis was collected from the same level (excavation at left).

Directions to Stop 2.4

Retrace the route back to the west and up to the CCC Road, ***note mileage***, and turn left to continue north (Fig. 8). The road generally follows just below the shoreline at 1850 m, and in several places provides great overviews of the 1843 m shoreline to the west (Fig. 12). After passing Hequy Well (~5 mi), where Lillquist (1994) obtained a date of 15,070 ± 100 ^{14}C yr B.P. from a lagoon east of the road, the road passes near a small cuspate spit formed as a paired of tombolos extended out to a small bedrock island while the lake stood at the 1840 m level (Fig. 13). North

Figure 12. The 1843 m shoreline below the CCC Road in northeastern Franklin Valley (view to the north). The broad crest of this shoreline extends northward away from the viewer, and is visible curving off to the northwest. This ridge is paralleled at a lower elevation to the left (west) by another shoreline representing the 1840 m water level. The crests of both ridges are accentuated by lighter-colored vegetation. See Figure 8.

of this point, the shoreline transitions from an isolated ridge to one plastered on the side of a bedrock upland. After ~8 mi, park alongside the road and hike downslope to the west to reach the bedrock outcrop for Stop 2.4.

Stop 2.4. Wave-Cut Platform at Lake Franklin Highstand (40.60479°N, 115.13465°W)

This stop provides an expansive overview across the northern end of the Franklin Valley, as well as access to a local erosional feature produced when the lake was at the 1850 m highstand (Fig. 13). At this location, Lake Franklin was nearly 12 km wide when the highstand shoreline was occupied, and maximum fetch for southerly winds exceeded 50 km. Production of substantial waves was possible in a lake of this size, and the flat surface eroded into the limestone bedrock at this location appears to be a wave-cut platform. Most of the highstand shoreline segments of Lake Franklin mapped by Lillquist (1994) are depositional, but 40% were classified as erosional, and Sharp (1938) also commented on wave-cut features in the basin. The surface of this outcrop is heavily weathered, but the overall effect of wave planation is visible. The elevation here is 1848 m, so water depths were on the order of 2–5 m during the highstand. Reconnaissance along the bedrock outcrop to the east of the road reveal rounded cobbles in the apron of sediment at the base of the bluff, suggesting that waves may have cut the bluff as a sea cliff. Lillquist (1994), however, notes that the presence of numerous faults in this area complicate identification of linear features related directly to lake activity.

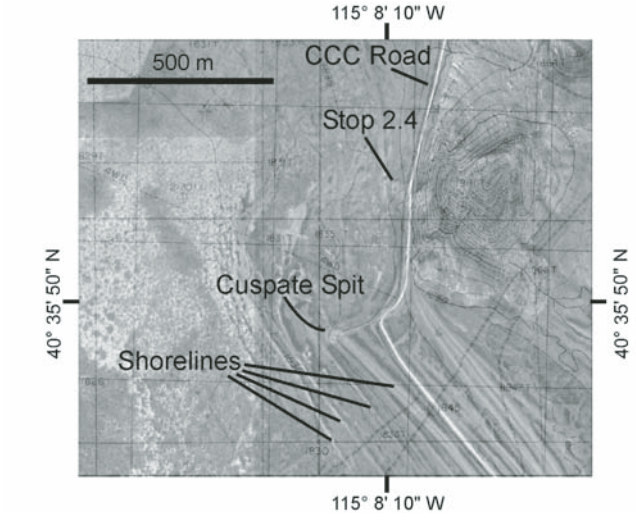

Figure 13. Aerial photograph overlain on topographic map showing part of the northeastern Franklin Valley (portion of the U.S. Geological Survey 7.5′ Smith Well quadrangle). The CCC Road followed by the field trip route is visible as the light-colored line. The wave-cut platform at Stop 2.4 is highlighted. Note the location of the platform where the highstand shoreline comes in contact with a bedrock-cored upland. The small cuspate spit connected to a bedrock outcrop at the 1840 m shoreline is also identified, along with numerous other shorelines (from 1840 m to 1830 m) visible at the southern extent of the map.

Directions to Stop 2.5

Hike back up to the vehicles and continue northward along the CCC Road. After 3 mi, the road passes through an old gravel quarry. Park near the north end of the quarry for Stop 2.5.

Stop 2.5. Deep Gravel Quarry on CCC Road (40.64649°N, 115.13791°W)

This final stop in the Franklin Valley focuses on a gravel pit where material was removed from a compound beach ridge for road construction. Lillquist (1994) describes the stratigraphy in a former exposure within this excavation where interbedded sandy gravel and gravelly sand were visible. Beach deposits of the highstand shoreline were originally present just east of this site, but have been largely mined away or disturbed by equipment. This sandy gravel was underlain by a gravelly sand interpreted as nearshore deposit representing regression from the 1850 m highstand. A thin layer (~10 cm) of sandy clay beneath the gravelly sand was interpreted as offshore clay representing the (short?) time when the water level was above this site, forming the highstand beach. This unit is underlain by another thin layer of gravelly sand representing foreshore deposits of the transgression to the highstand level.

The lowest unit of the exposure was sandy gravel heavily cemented by carbonate, and Lillquist (1994) reported the carbonate morphology to be equivalent to Stage IV (Birkeland et al., 1991). Given this level of development, he concluded that this gravel represents a much older beach deposited when an ancestor of Lake Franklin rose to this level earlier in the Pleistocene. Lillquist (1994) did not date this layer, but suggested that its age could approach 750,000 yr given the similarity of carbonate development to a site in southern Utah of that age.

In 2010, the authors obtained a shell sample from this cemented layer that was suitable for radiocarbon dating. The shell returned a date of 42,300 ± 480 ^{14}C yr B.P. (45,600 B.P.), indicating that the beach certainly predates the MIS-2 highstand, even if Lillquist's estimate is too old. It is unclear how this date should be interpreted. Taken at face value, it suggests that a lake stood near the level of the MIS-2 highstand during MIS-3. Little is known about pre–MIS-2 lakes in the Great Basin, although older shorelines have been reported from some basins. In most cases, the ages of these features are unknown; however, work with a long sediment core from the Bonneville Basin suggests, not surprisingly, that deep lakes formed during glacial periods (Oviatt et al., 1999). Extrapolating this conclusion westward, it seems unlikely that Lake Franklin would have stood near its highest level for MIS-2 during the interstadial of MIS-3. Maybe this sample failed to yield an accurate age because of aragonite to calcite recrystallization. In this scenario, the age should be viewed as a minimum limit, and the actual age of the carbonate-cemented gravel would be older

than 45,600 years, perhaps representing deposition by a high lake during MIS-4 or even MIS-6.

Directions to Stop 2.6

Continue north on the CCC Road a short distance to intersect NV-229. Turn right on this paved road and climb over the divide out of the Franklin Valley (Fig. 8). At the intersection with U.S.-93, ***set trip odometer to zero***, turn left (north), and descend into the Clover Valley (Fig. 14). The highstand of pluvial Lake Clover at 1729 m is crossed ~5.3 mi north of this intersection, although no shoreline feature is visible. The road continues down into the basin and passes near the western end of the Snow Water Lake playa (Bureau of Land Management [BLM] sign). An impressive set of dunes rises ~10 m above the playa surface to the southeast, while other dune ridges are visible along the north side of the playa in the distance. Continuing north on U.S.-93 watch for a right turn entering a gravel pit marked by a small BLM sign for "Tobar" ~19 mi north of the

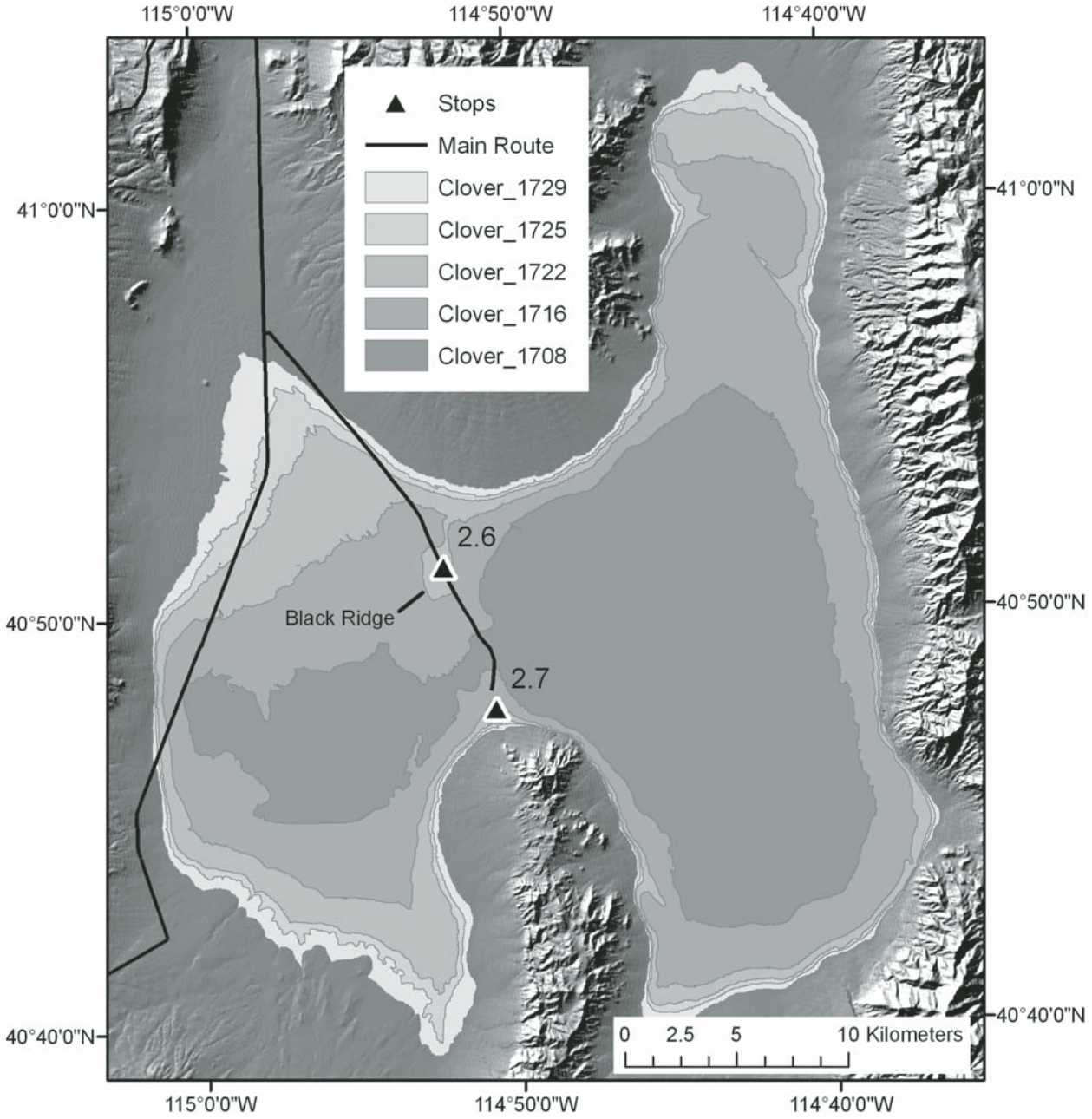

Figure 14. Map of the Lake Clover region with outlines of the lake at five different elevations (in meters). Field trip stops are identified, and the route of the trip (from Fig. 2) is shown.

U.S.-93 intersection. Turn here, pass through the gravel pit, and continue to follow the dirt road as it veers south following the railroad tracks into the Clover Valley. At a prominent intersection (25.5 mi) stay to the right on the west side of the tracks. The road continues southward, drops below the 1729 m shoreline, and runs parallel to a prominent ridge at 1716 m to the left. This ridge extends southward as a tombolo toward an upland known as Black Ridge. Follow the road to the crest of this upland (~29 mi) and park along the left after the fence marking the end of private property around a house trailer for Stop 2.6.

Stop 2.6. Black Ridge (40.85248°N, 114.87100°W)

Several shorelines of Lake Clover are preserved in the vicinity of Black Ridge, a low-relief, bedrock- (or gravel-) cored ridge that was an island near the north-central shoreline during the highstand of Lake Clover (Fig. 14). The highest elevation of Lake Clover (1729 m) is represented by a nearly continuous shoreline ridge along the broad alluvial fan in the north-central sector of the basin. Shoreline ridges representing regressive phases of the lake are also preserved here; the most continuous are at elevations of 1725, 1722, and 1716 m. Although the ages of the Lake Clover shorelines are not known, we have collected fossil mollusk shells from multiple sites in the valley that will provide ^{14}C age limits on shorelines at 1729, 1725, and 1716 m.

Directions to Stop 2.7

From the summit of Black Ridge continue south on the gravel road, dropping immediately below the shoreline from the Lake Clover highstand (Fig. 14). Depending on the light conditions, several subtle shoreline benches are visible as the road drops down to cross the (likely dry) channel known as "The Slough" that leads to a terminal basin in the Independence Valley east of the road. The road becomes finer and locally rutted at these lowest elevations, but should be passable unless it has recently rained. Approaching the northern extent of Spruce Mountain Ridge, the road rises up onto an impressive complex of shoreline features forming a series of nested cuspate spits. Stay left at the BLM signboard (33 mi), and then make a very sharp right on a two-track heading back to the west (34 mi). Park alongside the road for Stop 2.7.

Stop 2.7. Ventosa (40.79518°N, 114.84453°W)

Shorelines at the south-central end of Lake Clover are visible at this stop. Here, the most prominent shoreline feature (quite obvious on a topographic map or aerial photograph) is a V-shaped cuspate spit at 1715 m (Fig. 15). The gravel road trending northwest-southeast is built upon the eastern limb of this feature, while aerial photography reveals multiple ridges along the western limb of the spit that are cut by the

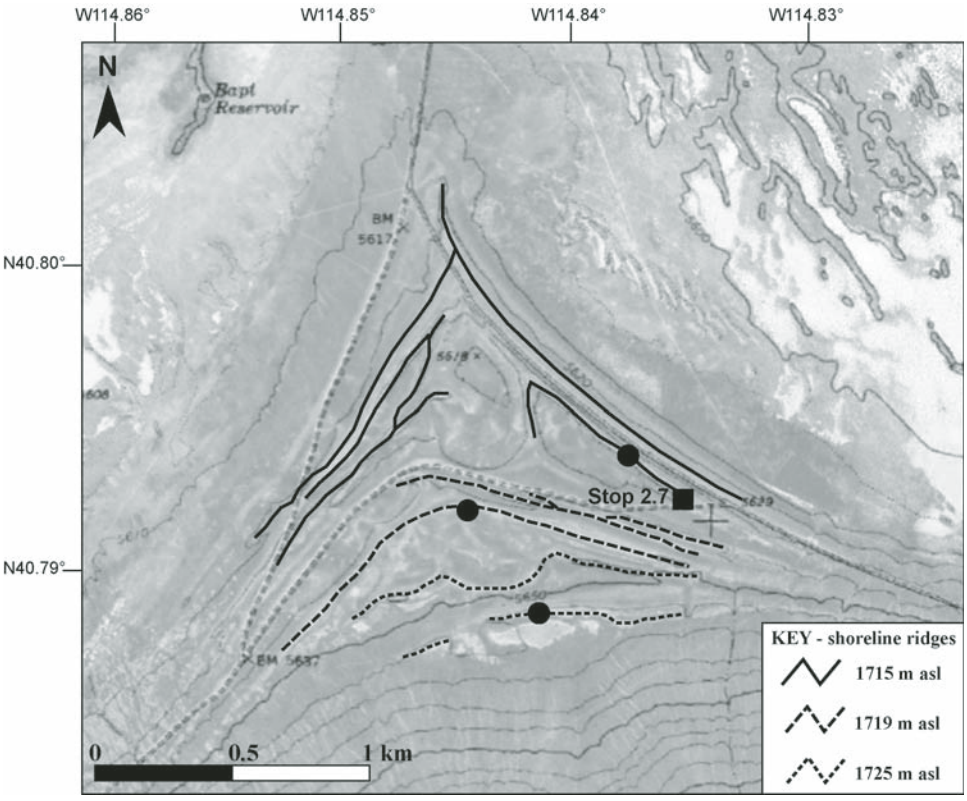

Figure 15. Shorelines of pluvial Lake Clover at the Ventosa area viewed at Stop 2.7 (portion of the U.S. Geological Survey 7.5′ Ventosa quadrangle). The highstand shoreline (1725 m) hugs the northern extent of the bajada extending from Spruce Mountain Ridge (south of figure). The next lower shoreline (1719 m) exhibits a transition to northward progradation. The lowest shoreline, at ~1715 m, forms a prominent V-shaped cuspate spit indicating that prevailing wind directions were driving sediment transport northward when the lake stood at this level. Circles indicate sites where trenches and/or auger holes were dug to sample deposits for optically stimulated luminescence and/or ^{14}C dating.

northeast-southwest–trending road. The center of the triangle was a lagoon when Lake Clover stood at the 1715 m level. To collect samples suitable for OSL dating from this landform, and to investigate its internal stratigraphy, a trench was excavated across the northwest-southeast–trending portion of the spit in 2008 with a backhoe. The trench exposed the upper 2 m of sediment over a distance of ~20 m along the back slope of the ridge, perpendicular to the trend of the spit (Fig. 16). The trench revealed that the spit is composed of thin beds of open-work gravel, gravelly sand and coarse sand, with clast sizes ranging from pebbles to small cobbles. Most beds are continuous over less than 5 m, and gently dip (<5°) toward the depression west of the spit. Clasts within 1 m of the surface display thin (<2 mm thick) secondary carbonate coatings on their undersides (Fig. 16).

No shells were found in the sediments exposed in the trench; however, OSL ages for the trench sediments range from 11.35 ± 2.76 to 8.68 ± 2.07 ka B.P. (Laabs and Munroe, 2009). We view these as minimum age limits because they are inconsistent with hydrographs for lakes in the nearby Franklin and Bonneville basins (e.g., Lillquist, 1994; Oviatt, 1997). Lake Bonneville fell below its outlet threshold by ca. 17,300 B.P. and experienced an overall decline in shoreline elevation after ca. 15,000 B.P. Based on the updated chronology of Lake Franklin shorelines presented earlier, water levels were falling after this time there too. Additionally, uncertainties in the time-integrated in situ water content of the shoreline deposits may significantly affect OSL ages. Although the stratigraphy of the spit sediments suggests continuous deposition during the lake stand at 1715 m, it is unclear how long the water level of Lake Clover remained at the elevation of the spit after it was deposited, or if the water level rose back up to this level at some point after the spit was first formed. Either way, the modern in situ water content could underestimate the long-term average, which would result in OSL ages younger than the true age of the spit. We are testing for systematic errors in these OSL ages by applying ^{14}C dating to the same shoreline ridges.

The orientation of the V-shaped cuspate spit and other shoreline features at this elevation suggests a prevailing southerly wind direction during the regressive phases of Lake Clover. Waves approaching from the south, southwest, or southeast were necessary for formation of the cuspate spit at this site (Fig. 15), the tombolo near Black Ridge (Fig. 14), and the long spit at the northeast end of the lake basin (Fig. 14), all of which are at ~1716 m. Although the age of this shoreline is not known, a southerly prevailing wind direction is contrary to westerly wind fields inferred from spit orientations and lake-circulation modeling for the regressive phases of Lake Bonneville, particularly for the Provo shoreline that spans 17.3–14.5 ka B.P. (Oviatt, 1997; Jewell, 2010). However, southerly winds are prevalent in the modern wind field of the northeastern Great Basin, becoming most powerful during storm events associated with low-pressure systems. If the modern wind field was established during the regressive phases of Lake Clover, then it is likely that the ~1716 m shoreline was formed at a time when regional circulation was no longer strongly affected by North American ice sheets, sometime after the global LGM, 20–19 ka.

Higher shorelines of Lake Clover are visible at this site too, as nearly continuous, low-relief ridges on the alluvial fan to the south (Fig. 15). The highest shoreline at 1729 m is composed of gravels and sands similar to those comprising the V-shaped cuspate spit. A 1-m-deep trench was excavated in this shoreline and samples were collected for OSL dating in 2009. Once again, OSL ages for this shoreline (ranging from ca. 4 to 6 ka) are likely too young. As a possible remedy, an extensive augering campaign on beach ridges and lagoons throughout the Clover Valley in 2010 yielded several samples of mollusc shells suitable for radiocarbon dating, including several from the 1729 m highstand. Results

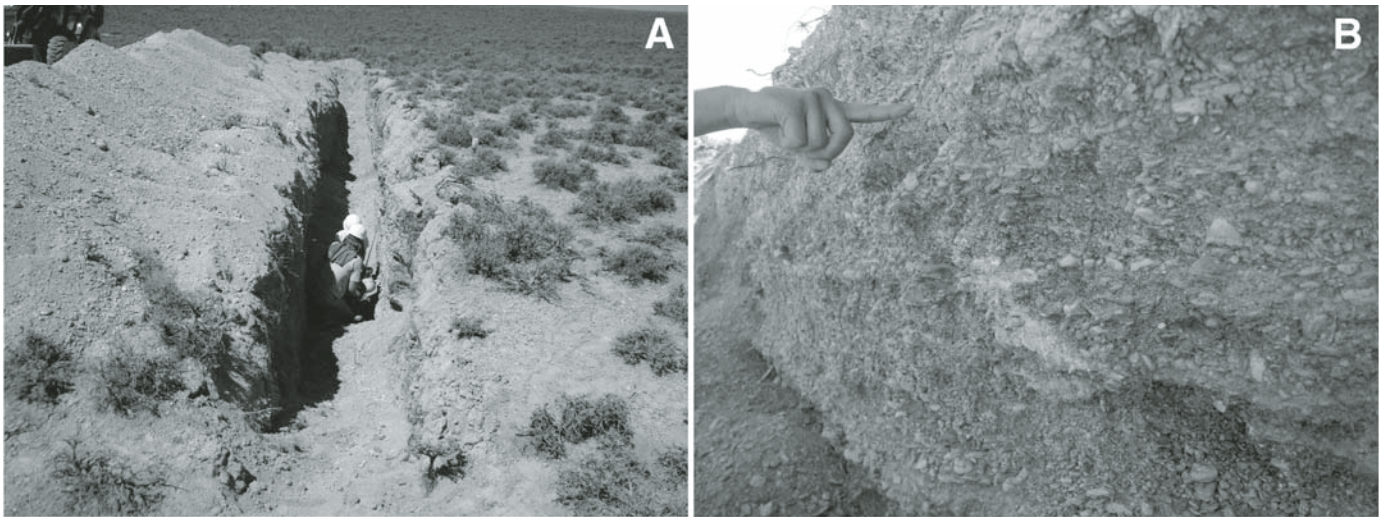

Figure 16. (A) The trench excavated by a backhoe in the eastern branch of the V-shaped cuspate spit at (~1715 m asl) the Ventosa site viewed at stop 2.7 (view in A is to southwest). (B) Sandy gravel and gravelly sands that comprise the spit and typify shoreline deposits of Lake Clover elsewhere in the basin.

from these analyses will hopefully help refine the ages of the main Lake Clover shorelines.

Directions to Elko

Retrace the route back out to U.S.-93 and turn right to head north to Wells. Pass under the highway and turn left to enter I-80 westbound. Continue west to Elko (47 mi) and take exit 303 to return to the Red Lion Hotel.

DAY 3. ELKO TO LOGAN: THE LAMOILLE TYPE LOCALITY AND LAMOILLE CANYON

(Driving distance: ≈260 mi/420 km.)

The final day of this trip will focus on the glacial geology of the Ruby Mountains (Fig. 2). After checking out of the Red Lion Hotel in the morning, we will head directly to the western side of the Ruby Mountains to visit the type locality for the Lamoille Glaciation, and the spectacular Lamoille Canyon. After lunch we'll head north to I-80 and then retrace our route to Logan across northwestern Utah.

Please note that the owners of the Ruby Dome Ranch have kindly provided access to their land for this field trip to visit the Lamoille type locality and Seitz Canyon. *This permission is not extended to future followers of this field trip route unless specific arrangements are made with the ranch owners.* Thus, Stops 3.1 and 3.2 should not be attempted by anyone seeking to replicate this exact itinerary. Fortunately, extensive views of the Lamoille deposits are visible from the road heading toward Lamoille Canyon that bisects the moraine belt.

Directions to Stop 3.1

From the Red Lion Hotel, turn right on Idaho Street and then left on 5th Avenue. Follow 5th Avenue as it curves left to become NV-227 toward Spring Creek. This road continues for ~19 mi toward the Ruby Mountains, providing tremendous views of the steep glacial valleys south of Lamoille Canyon. Depending on the

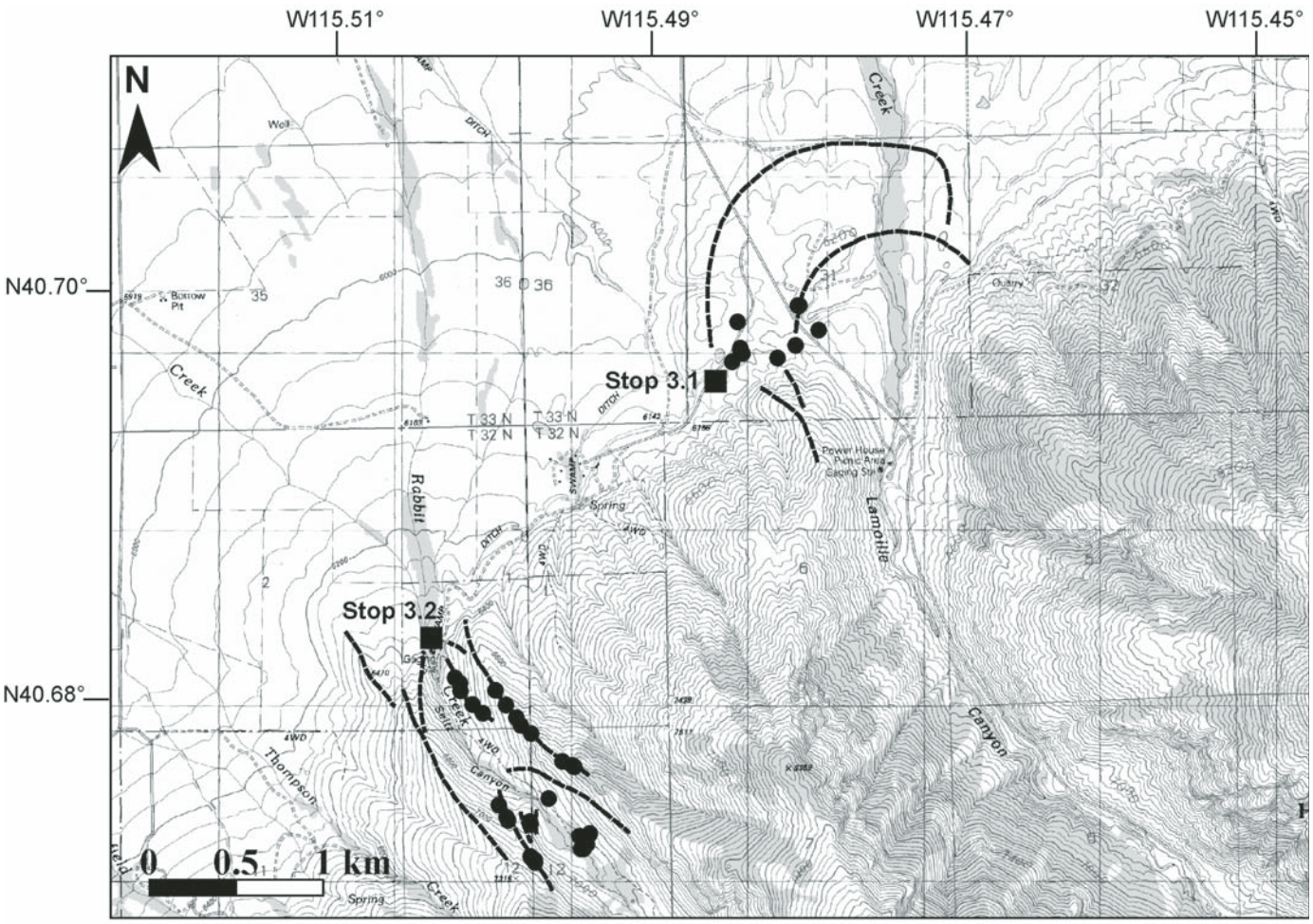

Figure 17. Topographic map showing the lower reaches of Lamoille and Seitz Canyons (portions of the U.S. Geological Survey 7.5′ Lamoille and Noon Rock quadrangles), including Stops 3.1 and 3.2 (squares). Dashed lines indicate mapped moraine crests, and circles indicate locations of boulders sampled for cosmogenic ^{10}Be surface-exposure dating.

light conditions, moraines of the Angel Lake Glaciation (arcuate ridges crossing the valleys at higher elevations) and Lamoille Glaciation (continuous lateral moraines at lower elevations) may be visible. After 19 mi, turn right on Lamoille Canyon Road and head south toward the range front. The road crosses a compound outwash surface deposited during multiple Pleistocene glaciations, and reaches deposits of the Lamoille type locality near the mouth of Lamoille Canyon (Fig. 17). The Ruby Dome Ranch is accessed through a gate on the right just inside the moraine belt. Close the gate behind the vehicles and descend the slope to the left. Park along the road at the base of descent, and hike upslope toward the prominent boulders for Stop 3.1.

Stop 3.1. Ruby Dome Ranch Road, Lamoille Type Locality (40.69815°N, 115.48804°W)

A broad, hummocky moraine at the mouth of Lamoille Canyon was designated the type locality for the Lamoille Glaciation by Sharp (1938), and is one of few locations in the Ruby and East Humboldt Ranges where moraines are preserved at the mountain front (Fig. 17). The lobate shape of the moraine suggests that it was formed by a piedmont glacier emanating from the mouth of Lamoille Canyon.

The Lamoille Glaciation has been correlated to the Illinoian Glaciation (MIS-6; 186–128 ka) based on weathering characteristics of moraines (Bevis, 1995; Wayne, 1984). However, cosmogenic ^{10}Be surface-exposure dating of Lamoille-age moraines at Hennan Canyon, a few km south of Stop 3.1, yielded ages ranging from ca. 19 to 66 ka, suggesting a younger age for the Lamoille Glaciation (Briggs et al., 2004). We sampled tall, quartz-rich boulders atop the type Lamoille moraine at this site (Fig. 18) along with clasts in outwash gravel that grades from the moraine for cosmogenic ^{10}Be surface-exposure dating. Moraine boulders display evidence of physical erosion at their surfaces; however, when combined with a depth-profile age of outwash gravel downvalley, cosmogenic exposure ages may provide more precise limits on the timing of the Lamoille Glaciation.

Figure 18. Large erratic boulder atop the type Lamoille moraine viewed at Stop 3.1 (view to the west). This boulder was sampled for cosmogenic ^{10}Be surface-exposure dating.

Directions to Stop 3.2

Return to the vans and continue along the road into the Ruby Dome Ranch (Fig. 17). At the house, turn left and park at the gate. Leave the vehicles, pass through the gate being sure to close it behind you, and hike south (right) along the two-track toward Seitz Canyon. At a stream gaging station near the canyon mouth (~0.9 mi) the two-track turns left and climbs up the canyon to the proximal slope of the prominent Lamoille-age right lateral moraine. Continue 0.75 mi to the Angel Lake moraine complex for Stop 3.2.

Stop 3.2. Seitz Canyon (40.38166°N, 115.50751°W)

Seitz Canyon was occupied by one of the largest valley glaciers in the Ruby Mountains during the Lamoille and Angel Lake Glaciations. The moraine sequence in this canyon is very well preserved, displaying prominent left- and right-lateral moraines mapped as Lamoille-equivalent that extend to the mouth of the canyon where they are offset by a normal fault (Fig. 17). In the canyon, Angel Lake–age moraines are inset to the prominent Lamoille-age lateral moraines. In both Seitz and Hennan Canyons, the Angel Lake terminal moraine displays three prominent ridge crests (Fig. 19), suggesting repeated occupation of the moraines during the last glaciation. Similar moraine morphology

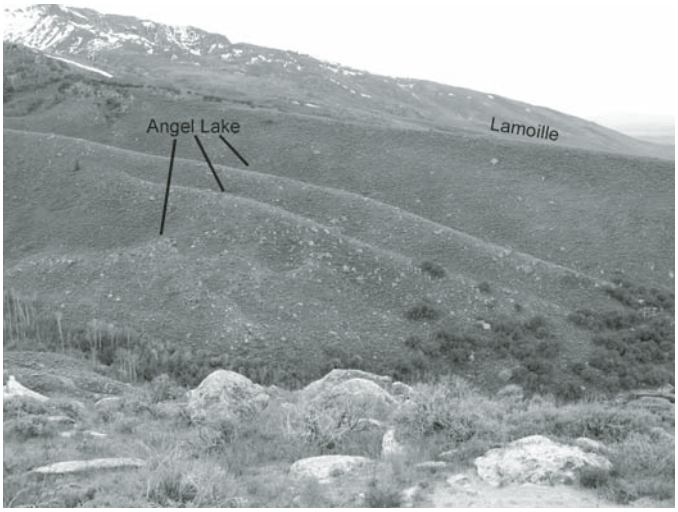

Figure 19. View southward across the lower part of Seitz Canyon moraines showing four different moraine ridges representing two different glaciations. The highest, longest ridge is a left-lateral moraine produced during the Lamoille Glaciation. The inner three moraines represent the Last Glacial Maximum Angel Lake Glaciation, which apparently involved multiple oscillations of the ice margin to produce these separate moraine crests. Samples from all of these moraines are being processed for cosmogenic ^{10}Be surface-exposure dating.

is observed elsewhere in the Great Basin; for example, in the Wallowa Mountains where glacier maxima were dated at ca. 21 ka and ca. 17 ka (Licciardi et al., 2004). We have sampled moraine boulders atop all three ridges of the Angel Lake terminal moraine complex and atop recessional moraines farther upvalley in Seitz Canyon for cosmogenic ^{10}Be surface-exposure dating.

Directions to Stop 3.3

Hike back to the vehicles and drive back out to the main road. Turn right to enter Lamoille Canyon (Fig. 17). Signs near the boundary of the Humboldt-Toiyabe National Forest announce the start of the Lamoille Canyon Scenic Byway, which extends for 12 mi up to Roads End at an elevation of 2675 m near the head of the canyon. Following along the north and east side of Lamoille Creek through a deep U-shaped valley, this road is one of the most scenic drives in the Great Basin. A picnic area near the canyon mouth (fee charged) provides a sheltered spot for lunch along the rushing waters of Lamoille Creek, while other pull-outs with interpretive signs along the way highlight important aspects of the canyon's scenery and natural history. Stop 3.3 is located 3 mi from the canyon mouth on the right. Park on the right in the prominent pull-out overlooking the hanging valley of the Right Hand Fork.

Stop 3.3. Confluence of Lamoille Canyon and the Right Hand Fork (40.66192°N, 115.43883°W)

An interpretive sign at this pull-out asks the question "What is a Glacier?" in front of a spectacular example of glacial geomorphology. Straight ahead to the south is the glacial valley of the Right Hand Fork which enters Lamoille Canyon as a hanging valley. During the Lamoille Glaciation, ice from both valleys met at this point and continued westward to the moraine position at the canyon mouth visited in Stop 3.1. Depending on light conditions, parallel downvalley-sloping benches interpreted as lateral moraines of Lamoille age are visible on the northern valley wall (behind you as you face the Right Hand Fork). During the more recent Angel Lake Glaciation, the glacier in Lamoille Canyon failed to reach this far down valley, and the glacier in the Right Hand Fork terminated as a piedmont lobe sprawled across the valley floor below the interpretive sign. The right lateral moraine of this glacier is an obvious ridge to the left rising nearly 100 m above the valley floor (Fig. 20). We have sampled boulders along the crest of this feature for ^{10}Be surface-exposure dating and processing is under way. This lateral moraine wraps around as a fragmented terminal moraine visible as a series of lower relief ridges below the road, and an extensive outwash valley train graded to this moraine extends downvalley to the right as a sagebrush-covered flat.

The prominent Angel Lake–age right lateral moraine represents a major impediment to Lamoille Creek. Today the creek descends through a narrow gorge squeezed between the moraine and the road just upstream from the interpretive sign. Above the moraine, the stream meanders through a low-gradient reach where significant aggradation has occurred. Exposures below the road reveal several meters of fine silt unconformably overlying rounded cobble gravel, suggesting slackwater deposition in an impoundment. Discovery of this exposure raised the exciting possibility that the slackwater sediments represented a lake that formed during the LGM when the Right Hand Fork Glacier occupied the right lateral moraine position. However, OSL dating of the basal silt overlying the cobble gravel returned an age of 2.83 ± 0.25 ka B.P., indicating that the lacustrine fill was deposited in the late Holocene. Perhaps beaver activity or slope processes produced a dam that temporarily held back the waters of Lamoille Creek. The suitability of this location for damming the stream was not overlooked by early settlers in this area; remnants of an artificial dam are visible just at the top of the cataract. However, projection of this elevation upstream reveals that the historic dam would not have impounded water to the elevation of the sampled sediments.

Directions to Stop 3.4

Return to vehicles and continue upvalley. Turn right at the entrance to Thomas Canyon Campground and park straight ahead on the left. Take care not to block access to the campground host's trailer, the registration board, or any of the campsites. Leaving the vehicles, walk into the campground across the bridge spanning a now-dry channel of Lamoille Creek. Continue straight ahead, crossing a bridge over the active channel, and head into the brush behind the outhouse on the left. Follow obvious game trails ~50 m east up to the crest of a bouldery ridge for Stop 3.4.

Figure 20. The ice-proximal slope of the Angel Lake–age right-lateral moraine deposited by the glacier entering Lamoille Canyon from the Right Hand Fork (view to the east). The moraine at this location is more than 85 m high and features a sharp crest studded with large boulders. Several of these have been sampled for cosmogenic ^{10}Be surface-exposure dating.

Stop 3.4. Confluence of Lamoille Canyon and Thomas Canyon (40.64921°N, 115.40557°W)

Rising up out of the brush just upstream from the Thomas Canyon Campground is a prominent moraine ridge studded with boulders. The genesis of this ridge is somewhat equivocal: it could be a right lateral moraine from a glacier entering the main valley from Thomas Canyon, it could be a medial moraine from a combined Thomas-Lamoille Canyon glacier as mapped by Bevis (1995), or it could be a terminal moraine from the Lamoille Canyon Glacier. The latter is appealing because there is no other candidate elsewhere in Lamoille Canyon for the terminal position of ice during the LGM. However, the morphology of the ridge, including the curvature of its upper section, seems to indicate that it was formed by ice exiting Thomas Canyon. Unfortunately, because the heads of both canyons are quite close to one another to the south, both glaciers were eroding the same rock types and there is no diagnostic erratic lithology that could be used to distinguish the glacier source area. This leaves a strange dilemma. Lamoille Canyon is the largest and best developed U-shaped valley in the Ruby Mountains. It hosted the longest glacier in the Great Basin during the penultimate Lamoille Glaciation. Yet, the position of the glacial terminus in this valley during the LGM Angel Lake Glaciation cannot be recognized. One explanation is that the moraine was entirely eroded away by subsequent meltwater activity and slope processes after the Angel Lake deglaciation. This explanation is somewhat undermined, though, by the tremendous preservation of the moraine ridges at the mouth of the Right Hand Fork. Another more likely explanation is that the moraine has been buried and obscured by focused deposition of post-glacial mass-wasting deposits. Numerous examples of debris fans are visible along the steep sides of the entire canyon, and Wayne (1984) mapped over a dozen of them between the canyon mouth and head. Perhaps the Angel Lake–age moraine is unlocatable because it was entombed within one of these debris fans. Interestingly, numerical modeling simultaneously applied to glaciers in Lamoille, Thomas, and the Right Hand Fork Canyons indicates that combinations of temperature and precipitation necessary for growth of the latter two glaciers would have driven the Lamoille Glacier to a position just upstream from the Thomas Canyon Campground (Wendler and Laabs, 2008), suggesting that the ridge above the campground may actually be the terminal moraine from the Lamoille Canyon Glacier.

Directions to Stop 3.5

Return to the vans, drive back out to the Lamoille Canyon Road, and turn right to continue upvalley. The moraine ridge visited at Stop 3.4 is briefly visible through the trees, after which the road progressively curves around to head more due south. In the vicinity of the Terraces Picnic Area (fee charged) ledges of striated bedrock are visible alongside the road. Processing of samples collected from these ledges for cosmogenic surface-exposure dating is under way and will hopefully provide some constraint on the timing of deglaciation in the upper valley. Near-vertical exposures feature striations overlain on a wavy erosional pattern that may represent P-forms generated by subglacial meltwater erosion. A major debris flow chute near the Terraces Picnic Area reactivated in June of 2010, locally burying the road in more than 5 m of sediment, and causing evacuation of the Thomas Canyon Campground for several days. Mobilization of sediment in this event was driven by rapid melting of a deep snowpack. Above the Terraces Picnic Area, the valley widens and views become more extensive as trees diminish in height. The road passes far below the hanging valley occupied by Island Lake on the right and ends at the "Roads End" parking lot. Park the vehicles here for Stop 3.5.

Stop 3.5. Roads End (40.60432°N, 115.37582°W)

From Roads End, the spectacular extent of the head of Lamoille Canyon is revealed (Fig. 21). The U-shaped cross section of the valley is plainly visible, and the high hanging valley of Island Lake is obvious to the left when looking downstream (north). A well-graded trail to Island Lake provides an easy 2-mi climb up into this cirque. About halfway up, the trail passes a bench formed by till that is likely a lateral moraine. This feature is located just below the bridge over the cataract draining from the lake at an elevation of 2824 m, indicating a former ice thickness of ~200 m in this part of the valley.

Roads End is the northern terminus of the Ruby Crest trail, which extends over 40 mi southward along the crest of the range to terminate in Harrison Pass near the pull-out where we stopped on Day 2 to view the Franklin Valley. The trail climbs southward from Roads End and leaves the Lamoille watershed at Liberty Pass, a narrow notch visible high to the south from the parking lot. The timing of the ultimate deglaciation in the headwaters of Lamoille Creek is poorly constrained; however, a bog-bottom date

Figure 21. Northward view of the U-shaped valley of Lamoille Canyon from below Liberty Pass. The road leading to the Roads End turnaround (Stop 3.5) is visible on the valley floor.

of 13,000 ± 900 ^{14}C years was reported from the vicinity of Roads End (Wayne, 1984). This date was obtained on bulk sediment, which undoubtedly contributes to the wide error factor and makes it difficult to interpret. Nonetheless, taking the date at face value and calibrating it to calendar years indicates that the upper part of Lamoille Canyon was deglaciated by 13,300–17,900 yr B.P.

Directions Back to Logan, Utah

From Roads End at the head of Lamoille Canyon, retrace the route back down to the canyon mouth. Continue out through the Lamoille-type moraines, and turn right on NV-227. Pass through the small town of Lamoille, and turn left at the end of town on Crossroads Lane. Turn right at the next section boundary on Clubine Road, and then follow this main road (gravel) as at zigzags generally northward along the range front. After ~17 mi from Lamoille, turn left on NV-229 (paved), and after 2 mi, turn right following signs for Starr Valley. Go ~10 more miles and turn right at the intersection in front of Starr Valley Community Hall. Follow this paved road ~8 mi to the Welcome interchange at I-80. Enter I-80 eastbound and retrace the route from Day 1 back to Logan. (Travel 35 mi east to exit 378. Follow NV-233 to the Utah line, and continue on U.S.-30 to I-84. Head east to I-15, and then exit to follow U.S.-30 to Logan.)

ACKNOWLEDGMENTS

Our work in northeastern Nevada has been supported by National Science Foundation grant NSF-P2C2-0902586 to Munroe, NSF-P2C2-0902472 to Laabs, NSF-BCS-0808861 to Munroe, and a Geological Society of America Quaternary Geology & Geomorphology Division Gladys W. Cole Memorial Research award to Laabs. Thanks to the Humboldt-Toiyabe National Forest and the Bureau of Land Management for permission to conduct this research on federal land. M. Badding, L. Best, M. Bigl, J. Johnson, C. Kruger, L. Luna, N. Taylor, and L. Wendler assisted in the field.

REFERENCES CITED

Antevs, E.V., 1948, The Great Basin, with emphasis on glacial and postglacial times; 3, Climatic changes and pre-white man: Bulletin of the University of Utah, v. 38, no. 20, p. 168–191.

Bartlein, P.J., Anderson, K.H., Anderson, P.M., Edwards, M.E., Mock, C.J., Thompson, R.S, Webb, R.S., Webb, T., III, and Whitlock, C., 1998, Paleoclimate simulations for North America over the past 21,000 years; features of the simulated climate and comparisons with paleoenvironmental data; Late Quaternary climates; data synthesis and model experiments: Quaternary Science Reviews, v. 17, no. 6–7, p. 549–585, doi:10.1016/S0277-3791(98)00012-2.

Benson, L.V., May, H.M., Antweiler, R.C., Brinton, T.I., Kashgarian, M., Smoot, J.P., and Lund, S.P., 1998, Continuous lake-sediment records of glaciation in the Sierra Nevada between 52,600 and 12,500 ^{14}C yr B.P: Quaternary Research, v. 50, no. 2, p. 113–127, doi:10.1006/qres.1998.1993.

Benson, L., Kashgarian, M., Rye, R., Lund, S., Paillet, F., Smoot, J., Kester, C., Mensing, S., Meko, D., and Lindström, S., 2002, Holocene multidecadal and multicentennial droughts affecting Northern California and Nevada: Quaternary Science Reviews, v. 21, no. 4–6, p. 659–682, doi:10.1016/S0277-3791(01)00048-8.

Bevis, K.A., 1995, Reconstruction of late Pleistocene paleoclimatic characteristics in the Great Basin and adjacent areas [Ph.D. dissertation]: Corvallis, Oregon, USA, Oregon State University.

Birkeland, P.W., Machette, M.N., and Haller, K.M., 1991, Soils as a tool for applied Quaternary geology: Salt Lake City, Utah, USA, Utah Geological Survey Miscellaneous Publication no. 91-3.

Bischoff, J.L., and Cummins, K., 2001, Wisconsin glaciation of the Sierra Nevada (79,000–15,000 yr B.P.) as recorded by rock flour in sediments of Owens Lake, California: Quaternary Research, v. 55, no. 1, p. 14–24, doi:10.1006/qres.2000.2183.

Blackwelder, E., 1934, Supplementary notes on Pleistocene glaciation in the Great Basin: Journal of the Washington Academy of Sciences, v. 24, no. 5, p. 217–222.

Blackwelder, E., 1931, Pleistocene glaciation in the Sierra Nevada and Basin Ranges: Geological Society of America Bulletin, v. 42, no. 4, p. 865–922.

Briggs, R.W., et al., 2004, Cosmogenic Be-10 ages of Angel Lake and Lamoille Moraines and late Pleistocene slip rate of the rangefront normal fault, Ruby Mountains, Basin and Range, Nevada: Eos (Transactions, American Geophysical Union), v. 85, no. 47, 2004 Fall Meeting Suppl., abstract G11A-0773.

Burr, T.N., and Currey, D.R., 1988, The Stockton Bar, in the footsteps of G.K. Gilbert, *in* Machette, M.N., ed., Lake Bonneville and neotectonics of the eastern Basin and Range Province; guidebook for field trip twelve: Salt Lake City, Utah, USA, Utah Geological Survey Miscellaneous Publication no. 88-1.

Currey, D.R., and Oviatt, C.G., 1985, Durations, average rates, and probable causes of Lake Bonneville expansions, stillstands, and contractions during the last deep-lake cycle, 32,000 to 10,000 years ago, *in* Kay, P.A., and Diaz, H.F., Problems of and prospects for predicting Great Salt Lake levels—Proceedings of a National Oceanic and Atmospheric Administration Conference, 26–28 March 1985: Salt Lake City, Utah, USA, University of Utah Center for Public Affairs and Administration, p. 9–24.

Enzel, Y., Wells, S.G., and Lancaster, N., 2003, Late Pleistocene lakes along the Mojave River, Southeast California, *in* Enzel, Y., Wells, S.G., and Lancaster, N., eds., Paleoenvironments and paleohydrology of the Mojave and southern Great Basin deserts: Geological Society of America Special Paper 368, p. 61–77.

Garcia, A.F., and Stokes, M., 2006, Late Pleistocene highstand and recession of a small, high-altitude pluvial lake, Jakes Valley, central Great Basin, USA: Quaternary Research, v. 65, no. 1, p. 179–186, doi:10.1016/j.yqres.2005.08.025.

Gilbert, G.K., 1890, Lake Bonneville: Reston, Virginia, USA, U.S. Geological Survey Monograph 1, 438 p.

Howard, K.A., 2000, Geologic map of the Lamoille Quadrangle, Elko County, Nevada: Reno, Nevada, USA, Nevada Bureau of Mines and Geology Map 125, scale 1:24,000 (http://www.nbmg.unr.edu/dox/m125plate.pdf).

Jewell, P.W., 2010, River incision, circulation, and wind regime of Pleistocene Lake Bonneville, USA: Palaeogeography, Palaeoclimatology, Palaeoecology, v. 293, no. 1–2, p. 41–50, doi:10.1016/j.palaeo.2010.04.028.

Kutzbach, J.E., 1987, Model simulations of the climatic patterns during the deglaciation of North America, *in* Ruddiman, W.F., and Wright, H.E., Jr., eds., North America and adjacent oceans during the last deglaciation: Boulder, Colorado, USA, Geological Society of America, Geology of North America, v. K-3, p. 425–446.

Laabs, B.J., and Munroe, J.S., 2008, Glacial and pluvial records of the Angel Lake glaciation in northeastern Nevada and inferences of latest Pleistocene climate: Geological Society of America Abstracts with Programs, v. 40, no. 6, p. 147.

Laabs, B.J.C., and Munroe, J.S., 2009, Developing the Late Quaternary record of pluvial Lake Clover, Northern Great Basin, USA (abst.): Transactions, American Geophysical Union, Fall Meeting 2009, abstract #PP11D-1351.

Laabs, B.J.C., Plummer, M.A., and Mickelson, D.M., 2006, Climate during the last glacial maximum in the Wasatch and southern Uinta Mountains inferred from glacier modeling; Quaternary landscape change and modern process in western North America: Geomorphology, v. 75, no. 3–4, p. 300–317, doi:10.1016/j.geomorph.2005.07.026.

Laabs, B.J., Bash, E.B., Refsnider, K.A., Becker, R.A., Munroe, J.M., Mickelson, D.M., and Singer, B.S., 2007, Cosmogenic surface-exposure age limits for latest-Pleistocene glaciation and paleoclimatic inferences in the American Fork Canyon, Wasatch Mountains, Utah, U.S.A: Eos

(Transactions, American Geophysical Union) v. 88, no. 52, 2007 Fall Meeting Supplement, abstract PP33B-1274.

Licciardi, J.M., Clark, P.U., Brook, E.J., Elmore, D., and Sharma, P., 2004, Variable responses of Western U.S. glaciers during the last deglaciation: Geology, v. 32, no. 1, p. 81–84, doi:10.1130/G19868.1.

Lillquist, K.D., 1994, Late Quaternary Lake Franklin; lacustrine chronology, coastal geomorphology, and hydro-isostatic deflection in Ruby Valley and northern Butte Valley, Nevada [Ph.D. dissertation]: Salt Lake City, Utah, USA, University of Utah.

Lindstrom, S., 1990, Submerged tree stumps as indicators of mid-Holocene aridity in the Lake Tahoe region: Journal of California and Great Basin Anthropology, v. 12, no. 2, p. 146–157.

Lips, E.W., Marchetti, D.W., and Gosse, J.C., 2005, Revised chronology of late Pleistocene glaciers, Wasatch Mountains, Utah: Geological Society of America Abstracts with Programs, v. 37, no. 7, p. 41.

Louderback, L.A., and Rhode, D.E., 2009, 15,000 Years of vegetation change in the Bonneville basin; the Blue Lake pollen record: Quaternary Science Reviews, v. 28, no. 3-4, p. 308–326, doi:10.1016/j.quascirev.2008.09.027 (Special theme: modern analogues in Quaternary palaeoglaciological reconstruction, p. 181–260).

Madsen, D.B., and Currey, D.R., 1979, Late Quaternary glacial and vegetation changes, Little Cottonwood Canyon area, Wasatch Mountains, Utah: Quaternary Research, v. 12, no. 2, p. 254–270, doi:10.1016/0033-5894(79)90061-9.

Mifflin, M.D., and Wheat, M.M., 1979, Pluvial lakes and estimated pluvial climates of Nevada, United States: Reno, Nevada, USA, Nevada Bureau of Mines and Geology, Bulletin 94, 57 p.

Munroe, J.S., and Laabs, B.J.C., 2009, A 7000-year Lacustrine Record from Angel Lake, Nevada (abst.): American Geophysical Union, Fall Meeting 2009, abstract no. PP23C-1419.

Osborn, G., and Bevis, K., 2001, Glaciation in the Great Basin of the Western United States: Quaternary Science Reviews, v. 20, no. 13, p. 1377–1410, doi:10.1016/S0277-3791(01)00002-6.

Oviatt, C.G., 1997, Lake Bonneville fluctuations and global climate change: Geology, v. 25, no. 2, p. 155–158, doi:10.1130/0091-7613(1997)025<0155:LBFAGC>2.3.CO;2.

Oviatt, C.G., Currey, D.R., and Sack, D., 1992, Radiocarbon chronology of Lake Bonneville, eastern Great Basin, USA: Palaeogeography, Palaeoclimatology, Palaeoecology, v. 99, no. 3–4, p. 225–241, doi:10.1016/0031-0182(92)90017-Y.

Oviatt, C.G., Thompson, R.S., Kaufman, D.S., Bright, J., and Forester, R.M., 1999, Reinterpretation of the Burmester core, Bonneville Basin, Utah: Quaternary Research, v. 52, no. 2, p. 180–184, doi:10.1006/qres.1999.2058.

Oviatt, C.G., Madsen, D.B., and Schmitt, D.N., 2003, Late Pleistocene and early Holocene rivers and wetlands in the Bonneville Basin of western North America: Quaternary Research, v. 60, no. 2, p. 200–210, doi:10.1016/S0033-5894(03)00084-X.

Phillips, F.M., Zreda, M.G., Benson, L.V., Plummer, M.A., Elmore, D., and Sharma, P., 1996, Chronology for fluctuations in late Pleistocene Sierra Nevada glaciers and lakes: Science, v. 274, no. 5288, p. 749–751, doi:10.1126/science.274.5288.749.

Plummer, M.A., and Phillips, F.M., 2003, A 2-D numerical model of snow/ice energy balance and ice flow for paleoclimatic interpretation of glacial geomorphic features: Quaternary Science Reviews, v. 22, no. 14, p. 1389–1406, doi:10.1016/S0277-3791(03)00081-7.

Reheis, M.C., 1999, Extent of Pleistocene lakes in the western Great Basin: Reston, Virginia, USA, U.S. Geological Survey Miscellaneous Field Studies MF-2323.

Reinemann, S.A., Porinchu, D.F., Bloom, A.M., Mark, B.G., and Box, J.E., 2009, A multi-proxy paleolimnological reconstruction of Holocene climate conditions in the Great Basin, United States: Quaternary Research, v. 72, no. 3, p. 347–358, doi:10.1016/j.yqres.2009.06.003.

Richmond, G.M., 1986, Stratigraphy and correlation of glacial deposits of the Rocky Mountains, the Colorado Plateau and the ranges of the Great Basin; Quaternary glaciations in the Northern Hemisphere: Quaternary Science Reviews, v. 5, p. 99–127.

Rosenberg, B.D., Bigl, M.F., Munroe, J.S., and Ryan, P.C., 2011, X-Ray Diffraction Analysis of Weathering Patterns in High-Elevation Glacial, Periglacial, and Eolian Sediments in Northern Nevada and Utah: Geological Society of America Abstracts with Programs, v. 43, no. 1, p. 114.

Russell, I.C., 1885, Geological history of Lake Lahontan, a Quaternary lake of northwestern Nevada: Reston, Virginia, USA, U.S. Geological Survey Monograph 11, 287 p.

Sharp, R.P., 1938, Pleistocene glaciation in the Ruby-East Humboldt Range, northeastern Nevada with abstract in German by Kurt E. Lowenstein: Journal of Geomorphology, v. 1, no. 4, p. 296–323.

Simpson, J.H., 1876, Report of explorations across the Great Basin of the Territory of Utah for a direct wagon-route from Camp Floyd to Genoa, in Carson Valley, in 1859, by Captain J. H. Simpson (1876): U.S. Government Printing Office, Washington, D.C., USA, 518 p.

Thompson, R.S., 1992, Late Quaternary environments in Ruby Valley, Nevada: Quaternary Research, v. 37, no. 1, p. 1–15, doi:10.1016/0033-5894(92)90002-Z.

Wayne, W.J., 1984, Glacial chronology of the Ruby Mountains–East Humboldt Range, Nevada: Quaternary Research, v. 21, no. 3, p. 286–303, doi:10.1016/0033-5894(84)90069-3.

Wendler, L.C., and Laabs, B.J.C., 2008, Reconstructions of latest Pleistocene glaciers and paleoclimate in the Ruby–East Humboldt Mountains, Nevada, USA: Geological Society of America Abstracts with Programs, v. 41, no. 3, p. 25.

Manuscript Accepted by the Society 23 February 2011